1969

The adhesion of gold to aluminum oxide

James L. Brandner
Lehigh University

THE ADHESION OF GOLD TO ALUMINUM OXIDE

by

James LeRoy Brandner

A Thesis

Presented to the Graduate Committee

of Lehigh University

in Candidacy for the Degree of

Master of Science

in Metallurgy and Materials Science

Lehigh University

1969

CERTIFICATE OF APPROVAL

This thesis is accepted and approved in partial fulfillment of the requirements for the degree of Master of Science.

May 16, 1969
Date

Robert B Runke
Professor in Charge

G. P. Candidi
Chairman of the Department
of Metallurgy and Materials
Science

ACKNOWLEDGMENTS

The author wishes to express appreciation to Professor R. B. Runk of Lehigh University and Dr. D. J. Shanefield of Western Electric Company for their consultation and guidance in the preparation of this thesis .

The author is gratefully indebted to the Western Electric Company for the sponsorship of this investigation.

The author wishes to express thanks to the following members of the staff of the Engineering Research Center: G. E. Crosby and M. J. Andrejco for occasional assistance in the laboratory, R. E. Mistler, J. R. Piazza, and J. A. Burns for helpful discussions and as sources of references, H. H. Bierenfeld and R. P. Scherer for suggestions and construction of fixtures, W. H. Fisher for assistance in obtaining reference material, S. J. Buzash for cooperation in the use of the metallography laboratory, J. D. Nohe and K. L. Morton for analysis of samples, J. A. Carnevale for cooperation in preparation of slides, and P. A. Renzo and M. Dinges for preparation of the manuscript.

The author wishes to express special thanks to B. S. Madsen for his excellent optical photomicroscopy and to R. E. Woods for his excellent surface replication and electron photomicroscopy, both of which were indispensible to this thesis.

Above all, the author wishes to acknowledge the cooperation and understanding of his wife who contributed immeasureably to the project.

TABLE OF CONTENTS

LIST OF TABLES

LIST OF FIGURES

ABSTRACT

The adhesion of gold to sapphire has been investigated in an effort to develop a bonding model for the Au/Al_2O_3 system. Ultra-pure (99.999%) gold was bonded to sapphire by melting it on sapphire disks in a furnace with a controlled atmosphere. The tensile strengths of the bonds were measured by performing a pull test on the sessile drops using a specially designed fixture in an Instron testing machine. By varying the time, temperature, and atmosphere in the furnace, tensile strengths as high as 10,000 psi were obtained. An oxygen atmosphere was found to be necessary for the formation of strong bonds. A bonding model was developed based on van der Waals dispersion forces. Mathematical analysis of the system has led to an equation for the tensile strength of a bond formed in an oxygen atmosphere as a function of soak time and temperature. The increase in tensile strength of the Au/Al_2O_3 bond is a diffusion controlled process and measurements of the rate of increase has led to a calculation of the oxygen self diffusion coefficient in sapphire at 1100°C, 1150°C, and 1200°C. The observed dependence of the diffusion coefficient on temperature has led to a determination of the activation energy for ion mobility that agrees well with the value given by Kingery and Oishi. The equations predict that extremely high values of tensile strength are possible and that the results also apply to polycrystalline substrates.

I. INTRODUCTION

In recent years the formation of strong, adherent ceramic-to-metal seals has achieved increasing importance in industry. The manufacture of reliable ceramic-to-metal seals for electronic components, the reinforcement of engineering metals and alloys with sapphire whiskers, and the increasing use of thin films in electronic circuits have led to efforts to determine the mechanism of bond formation in several types of metal/ceramic systems. Since it is of interest to the electronics industry and because of the special physical and chemical properties it possesses, the Au/Al_2O_3 system has been chosen for this investigation. It is the purpose of this study to quantitatively investigate the bonding mechanism between gold and aluminum oxide.

II. LITERATURE REVIEW

The earliest studies of adhesive bonding between metals and ceramics were conducted in connection with investigations of procelain enamel coatings on steel and glass-to-metal seals for incandescent lamps.

In the late 1930's and early 1940's, the development of high power, high frequency electronic components made necessary the development of strong, vacuum tight, high temperature ceramic-to-metal seals. Techniques were developed for brazing metals to the specially prepared surfaces of ceramics. The surface preparation consisted of metallizing the ceramic surface with a metal that could be wet by a suitable brazing alloy. The metallizing was most often done by firing mixtures of molybdenum and manganese on the surface of the ceramic in a controlled atmosphere. The importance of being able to make a reliable seal led to an extensive effort to determine the important parameters of the process.[1-21] Since these important parameters depend on the bonding mechanism, attention was focused on determining the mechanism or mechanisms which controlled the bonding of the metallized layer to the ceramic substrate.

The results of many investigations of this type of ceramic-to-metal seal indicate that the mechanism is quite complicated. It appears that glass migration across the interface,[14] chemical reactions,[5,7] and intermediate phase formation[18,19] play a part in the process of bond formation and their relative importance depends in a complex way upon such variables as ceramic composition,[4,5,6,14,15]

surface roughness,[14] firing temperature,[4,5,6,14] atmosphere,[5,7,12,17,20,21] and previous processing history.[15]

Since the late 1950's, there has been much interest in developing high strength structural materials by reinforcing a metal matrix with sapphire filaments or whiskers. In order for this technique to work, it is necessary to be able to form strong bonds between the matrix material and the sapphire. Accordingly, many studies concerning the adhesion of engineering metals and alloys to sapphire have been undertaken.[22-34] The results of these studies have led many investigators to conclude that the mechanism of bonding is a chemical reaction in which one or more components of the alloy react with the aluminum oxide leading to a thin third phase boundary layer.[28,32] The apparent strength of the bond depends in a complex way upon such factors as the degree of chemical reaction[26,28,32] and the stresses at the interface due to thermal expansion mismatch.[29,30,31,32]

The method usually used to study the bonding in this type of metal/ceramic system is the sessile drop technique. The primary reason for this is that thermodynamic relations have been established between several of the drop parameters and the work of adhesion (See Appendix II). Through the efforts of several investigators[22-27] a body of data concerning the drop parameters for several metal/ceramic systems has resulted. An extensive effort has been expended to relate the work of adhesion to the observed adhesive strength of the components of these systems. Unfortunately, most systems studied do not lend themselves to such considerations either because one or more

of the critical requirements for the validity of the equations are not met or because of the difficulty in measuring the work of adhesion. In addition, these thermodynamic relations apply to energies, not stresses, and the energies of the bond are usually of less practical interest than the stresses that the bonds will support.

Metallizing ceramics with noble metals has long been used as a decorative process, but in recent years it has been achieving greater technological importance. With the development of the transistor followed closely by the mass production of integrated circuits, it has become apparent that entirely new techniques of interconnecting circuit components must be developed if full advantage is to be taken of the small size, high reliability, and low cost of the newer solid state devices. One such technique is the interconnection of these devices with thin film conductors. The interconnections produced in this process are films of gold (or, in some cases, tantalum) a few mils wide and several hundred angstroms thick supported by a suitable substrate. In order that the product operate reliably, the insulating substrates are subject to severe requirements: low electrical conductivity (especially surface conductivity), high thermal conductivity, smooth surface, high strength, low cost, and the ability to form strong adhesive bonds with the metal of the conductors. The two most common substrates having an acceptable compromise of these characteristics are glass substrates and high alumina substrates.

The importance of the adhesive bond has led efforts to determine the important parameters affecting the adhesion of thin films to

ceramics.[35-48] There appear to be several types of boundary formed between thin films and their substrates: mechanical boundaries on rough substrates; monolayer to monolayer boundaries when little or no diffusion or chemical reaction takes place; compound boundaries with a third phase boundary layer such as an intermetallic compound or an oxide; diffusion boundaries, and pseudo-diffusion boundaries formed when the metallic atoms impinge on the substrate surface with enough energy to penetrate several atomic layers into the solid.[45] The number of different types of boundaries indicates that there are several possible bonding mechanisms that can operate in the adhesion of thin films to ceramics. However, it has been determined that the measured strengths of the bonds between thin films and their substrates depend upon such factors as type of boundary,[45] the atmosphere* in which the film was deposited,[48] and the stress state of the system.[42]

Unfortunately, the study of bonding in thin films has been severely handicapped by the lack of a testing procedure that will yield results that are easily interpreted.[37,40,43,47]

The net result of all the studies of metal/ceramic adhesion is that several bonding mechanisms have been proposed and several important parameters have been isolated. However, due to the complexity

---

*It should be noted by the reader that the effect of atmosphere on the bonding of thin films to ceramic substrates is probably unrelated to the effect studied in this investigation.

of the bonding mechanism in the systems studied, the lack of a testing procedure that will yield results that are easily interpreted, and a lack of knowledge of exactly what forces are required to break a particular type of bond, it has not been possible in most cases to be able to formulate a bonding mechanism in enough detail to be able to predict the stresses a bond will support in a given situation.

III. EXPERIMENTAL

In order to quantitatively characterize the adhesive bonds in a metal/ceramic system care must be taken to choose a system in which a single bonding mechanism operates that is susceptible to mathematical analysis. In addition, if the sessile drop technique is used, the following advantages are afforded:

(1) Frozen sessile drops have a shape that is suitable for gripping with a fixture for performing a pull test, thus enabling the tensile stresses the bond will support to be measured without prior disturbance of the interface as would be the case in a soldering operation.

(2) Information can be gained about the surface and interfacial energies of the system from the shape of the drop.

(3) Sessile drop experiments can be done without elaborate experimental apparatus.

Further, a system that is stable in a laboratory atmosphere, forming gas, noble gases, nitrogen, and oxygen at temperatures up to and somewhat above the melting point of the metal would offer the following advantages:

(1) Vacuum or protective atmosphere would not have to be provided.

(2) It would be possible to use temperature and atmosphere as variables.

With the objective of keeping the number of variables to a minimum, the following requirements are also essential:

(1) There should be very little chemical reaction between the metal and ceramic.

(2) The surface of the substrate should be smooth enough so that mechanical interlocking is not a significant contributor to the overall bond strength.

(3) The metal should have a low yield strength at the testing temperature so that no appreciable stresses would be supported at the interface due to thermal expansion mismatch.

(4) The metal and ceramic should resist crack propagation.

(5) The system components should be available in very pure form.

(6) The system components should not be attacked by cleaning solutions.

Certainly no system could be expected to perfectly meet all of these conditions. However, it was decided that the system Au/Al_2O_3 had an acceptable compromise of these requirements.

The aluminum oxide substrates were chosen in the form of sapphire disks 1/8" thick, cut with a diamond wheel from a 1/4" diameter rod purchased from the Sapphire Products Division of the Adolf Meller Company in Providence, Rhode Island. In order to hold the disks when performing pull tests, they were ground so that they would fit into a dove tail slot with base angles of 76^{o} in a holding fixture.

The as-cut faces of the sapphire disks were far too rough to be suitable for a bonding surface so the disks had to be polished using the following procedure:

(1) rough grinding using a 6 μ diamond embedded wheel.

(2) polishing with 9 μ diamond paste.

(3) polishing with 3 μ diamond paste.

The same sapphire disks were used in successive experimental runs after they were repolished using only step (3) unless a small flake of sapphire was removed from the surface, then steps (2) and (3) were repeated. If a large flake of sapphire were pulled from the disk, the gold was placed in a smooth area for the next run. If there was not a large enough smooth area remaining, the disk was discarded.

The gold was 99.999% pure gold wire 1 mm in diameter purchased from Electronic Space Products, Inc., Los Angeles, California and 99.999% gold splatters purchased from Semi-Elements, Inc., Saxonburg, Pennsylvania. The optical emission spectroscopy analysis of the materials taken in the Materials Analysis and Characterization Laboratory of the Western Electric Company Engineering Research Center appears in the following table.

TABLE 1

ANALYSIS OF MATERIALS USED

	Sapphire	Wire	Splatters
Detected	Al	Au	Au
	Mg, Si trace	Mg, Ca trace	Si, Fe, Mg Fine
	Fe, Ca, T_i fine trace	Fe, Cu fine trace	Cu, Ag, Sn, P_b trace
Not Detected	Cd	Cd	Cd
	Ba	Ba	Ba
	Be	Be	Be
	As	As	As
	Na	Na	Na
	Sr	Sr	Sr
	Co	Co	Co
	Pd	Pd	Pd
	Cr	Cr	Cr
	Mo	Mo	Mo
	Zr	Zr	Ca
	Cu	Ge	
		Si	
		Ga	
	W	W	W
	B	B	B
	Mn	Mn	Mn
	Sb	Sb	Sb
	Zn	Zn	Zn
	Pb	Pb	Zr
	Sn	Sn	Ni
	V	V	V
	Bi	Bi	Bi
	Pt	Pt	Pt
	Ni	Ni	Ti
	Ag	Ag	
		Ti	

The furnace used for firing the specimens is an Engelhard horizontal, platinum wound, muffle tube furnace. This furnace is equipped to fire specimens in non-corrosive, non-poisonous, and non-explosive atmospheres at temperatures up to 1500^{o}C. A Barber-Coleman furnace Controller was used to provide temperature programming. The entire apparatus is located in the ceramics laboratory model shop, a clean room. The contact angles of the sessile drops were measured by means of a reticle mounted on the eyepiece of a stereo microscope and graduated in 5^{o} intervals.

The pull tests were done in an Instron testing machine using specially designed fixtures built in the Research Center Model Shop and shown in Figure 1. The sapphire substrates fit in a dove tail slot which is in a fixture mounted on the movable crossbar of the Instron machine. The fixture is designed so that it is movable in the direction perpendicular to the slot direction and pull axis. Thus, the center of the drop can be moved into the pull axis of the testing machine. The gold drop was gripped by a fixture that hangs from the load cell. The gripping fixture was designed so that it could grip drops of varying sizes and always pull perpendicular to the interface.

Each experimental run consisted of from seven to nine adhesion couples, i.e., gold/sapphire specimens. Before being put into the furnace, the specimens were subjected to the following cleaning procedure:

(1) Immersion in a cold 50-50 solution of concentrated HCl and deionized water.

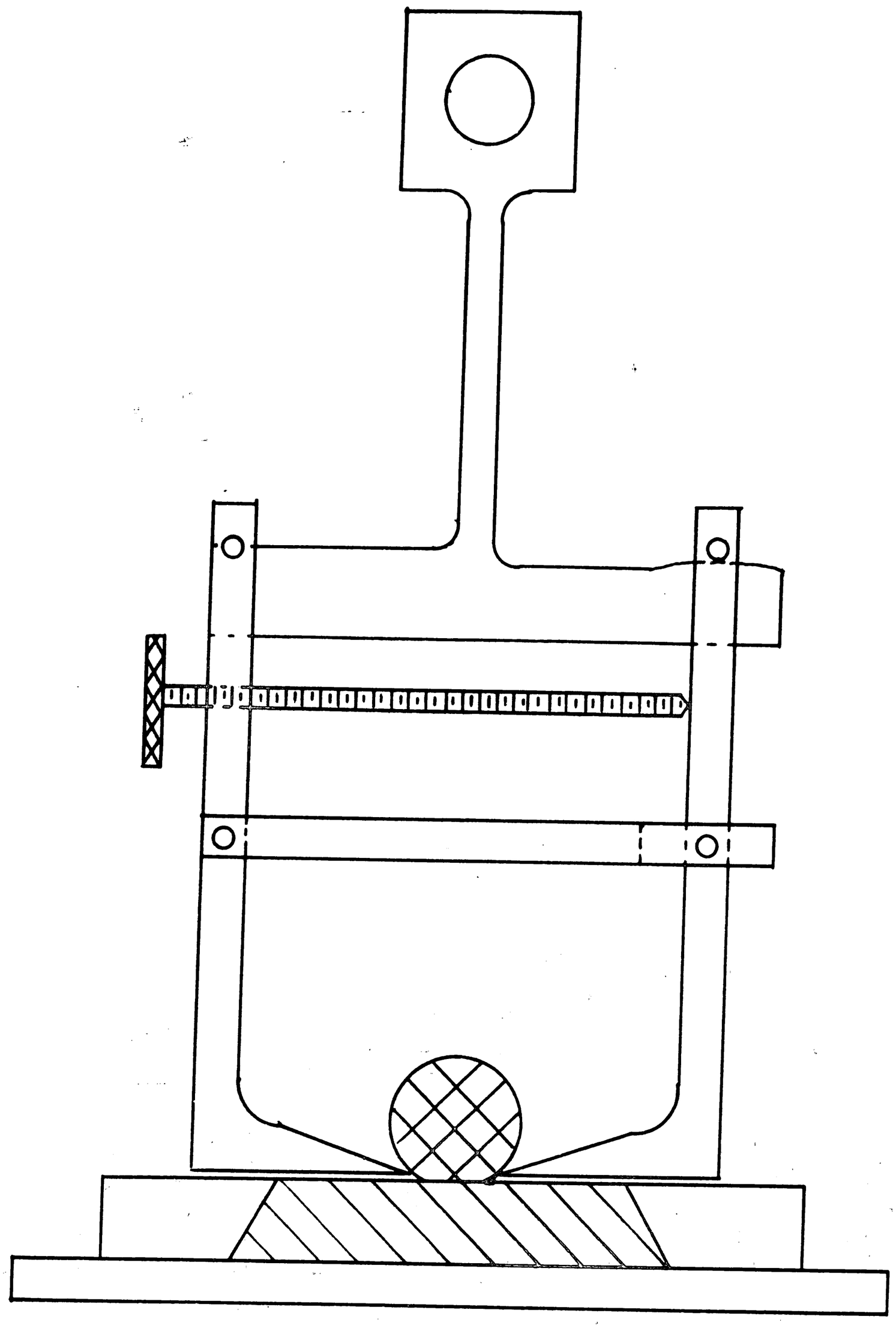

Figure 1
Tensile Testing Fixture.

(2) Rinse in a stream of deionized water.

(3) Rinse in a stream of J. T. Baker Chemical Company specially denatured Alcohol #3-A.

(4) Drying in a warm air stream.

(5) Ultrasonic cleaning in a proprietary detergent solution, Crystal Clean 513.

(6) Repeat of steps (2) - (4).

The cleaned specimens were placed on a D tube with tweezers and the tube pushed into the hot zone of the furnace. The end of the tube was sealed and the required atmosphere passed through the furnace at three liters per minute. This gas, except for nitrogen, was supplied by Air Reduction Company. Nitrogen was taken from a large tank of Natural Gas Cylinder Company liquid nitrogen. The gas was passed over a drying agent and piped into the furnace. The temperature controller was then programmed for the desired cycle. This cycle consisted of heating at an average rate of 2.4 ^{o}C per minute, holding for the desired time at a particular temperature, and cooling to 350 ^{o}C or below at an average rate of 1.7 ^{o}C per minute. The specimens were removed from the furnace, the contact angle measured, and the pull test performed using a crossbar speed of .1" per minute. To assure that the grip was not moved during the tightening around the gold drop, a plumb bob was suspended in front of the fixture and the drop lined up under it before pulling.

The maximum tensile stress was computed by dividing the breaking force in pounds by the area of the interface in square inches. The

area of the interface was measured by using a reticle mounted on a 3X lens. All systems used in these experiments had a nearly circular interface approximately one tenth inch in diameter.

The interfaces were examined microscopically after pulling and observations such as sapphire pullouts, gold stuck to the sapphire disks, distortion and gas occlusions in the gold drops were recorded.

The sapphire disks were repolished and recleaned and the gold drops recleaned unless they had pulled a sapphire flake from the disk, and the next run started.

IV. RESULTS

A. Tensile Strength Determinations

The research of Moore and Thornton[49] indicates that oxygen has a significant effect on the adhesive bond in the Au/SiO_2 system. To determine whether a similar effect would be observed in the Au/Al_2O_3 system six experimental runs, usually nine samples per run, were made at 1100°C for approximately one hour, three with an oxygen atmosphere and three with a nitrogen atmosphere. . The results appear in Table 2.

TABLE 2

TENSILE STRENGTHS (PSI) OF SPECIMENS FIRED AT 1100°C FOR 1 HOUR

Atmosphere	Sample Size	Mean	Std. Dev.
Oxygen	26	2150	434
Nitrogen	24	1630	544

For a complete listing of the data tabulated in Table 2 see Appendix III.

The mean of the tensile strengths of the adhesive bonds in the oxygen fired samples is significantly higher than that for the nitrogen fired samples at a 95% confidence level.

To ascertain further the effect of atmosphere three runs of usually seven samples each were devoted to the following experiment: After the usual cleaning procedure seven sapphire disks were lined up under a 1/8 inch sapphire rod which was supported on both ends by high purity sintered alumina setters. Seven lengths of gold wire were looped over the sapphire rod, one above each of the sapphire disks. The furnace temperature was raised and the system allowed to soak for 1/2 hour

at 1000°C in an oxygen atmosphere. The atmosphere was switched to nitrogen and the temperature raised to 1100°C and held for one hour. The data from these experiments is presented in Table 3.

TABLE 3

TENSILE STRENGTHS (PSI) OF SPECIMENS PREHEATED IN OXYGEN, MELTED IN NITROGEN, AND HELD FOR ONE HOUR AT 1100°C

Sample Size	Mean	Std. Dev.
20	1480	329

For a complete listing of the data tabulated in Table 3 see Appendix III.

The mean tensile strength of the bond in the specimens from this experiment was not significantly different from that of the samples fired in nitrogen.

To determine the effect of a reducing atmosphere on the formation of adhesive bonds, a run of five samples was made in a forming gas (90% N_2, 10% H_2) atmosphere by suspending five gold wires above five sapphire disks and raising the temperature to 1100°C for one hour. The tensile strengths of all bonds were negligible.

There is a striking difference in appearance among samples fired in oxygen, nitrogen, and forming gas. The specimens fired in oxygen are very bright and the gold drop is smooth. The specimens fired in nitrogen are rather dull and the gold drop has an uneven surface. The specimens fired in forming gas are very dull and the gold drops have an irregular shape with an elliptic interface.

Contact angles of specimens fired in oxygen were measured to be $120^{o} \pm 5^{o}$, those fired in nitrogen were measured to be $125^{o} \pm 5^{o}$, and those fired in forming gas varied from 125^{o} to 155^{o}, depending on where the measurement was taken.

The remainder of the experimental work concentrated on determining the effect of time and temperature upon the tensile strength of the bonds made in an oxygen atmosphere. Since it was reasoned that any perturbation of the tensile test results would always be in the direction of lower tensile strength, the specimen supporting the highest tensile stress in a given run was taken to be closest to the true tensile strength of a bond formed under those conditions of time and temperature. The highest tensile stress for each set of experimental conditions is given in Table 4.

TABLE 4

MAXIMUM TENSILE STRESS OBSERVED FOR EACH TIME AND TEMPERATURE

$1100^{o}C$

t (sec)	3600	15,000	27,000	33,600
$\sigma_{max}\left[\frac{lb}{in^2}\right]$	2860	6000	7380	7990

$1150^{o}C$

t (sec)	3600	4200	4980	5400	7680	16,200	24,000
$\sigma_{max}\left[\frac{lb}{in^2}\right]$	4610	3660	3760	3340	4200	4740	7620

$1200^{o}C$

t (sec)	3600	5100	5700	6900	7800	9900
$\sigma_{max}\left[\frac{lb}{in^2}\right]$	7040	9750	5360	3860	5100	5660

For a complete listing of the data from these experiments see Appendix III.

The 1100°C data is plotted in Figure 2. The data for 1150°C and 1200°C are plotted in Figure 3. The 1100°C data and theoretical considerations to be discussed in the next section indicate that these data should lie on smooth curves.

The dashed curves in Figure 3 show the deviation of the higher temperature data. A possible explanation for the failure of the points to lie on the curves at longer times is given in the discussion section.

It should be pointed out here that the fixture for pulling the gold drops from the sapphire substrate was designed for a maximum expected tensile stress of 3000 PSI. It was therefore not capable of pulling drops from their substrates when the bonds had a tensile strength greater than 5000 PSI and had only marginal success with those above 3000 PSI.

Hence, the higher values of tensile stress were measured indirectly by means of a shear test as performed by Moore and Thornton.[49] Nicholas, Forgan, and Poole[33] show that for the nickel/sapphire system the magnitude of the shear strength of the bond is about 90% of the magnitude of the tensile strength when the contact angle is less than 107°. Since all the gold drops plastically deformed during the shear test so that the effective contact angle was 90°, the shear test results were converted to tensile test results by dividing them by 0.9 as a first approximation.

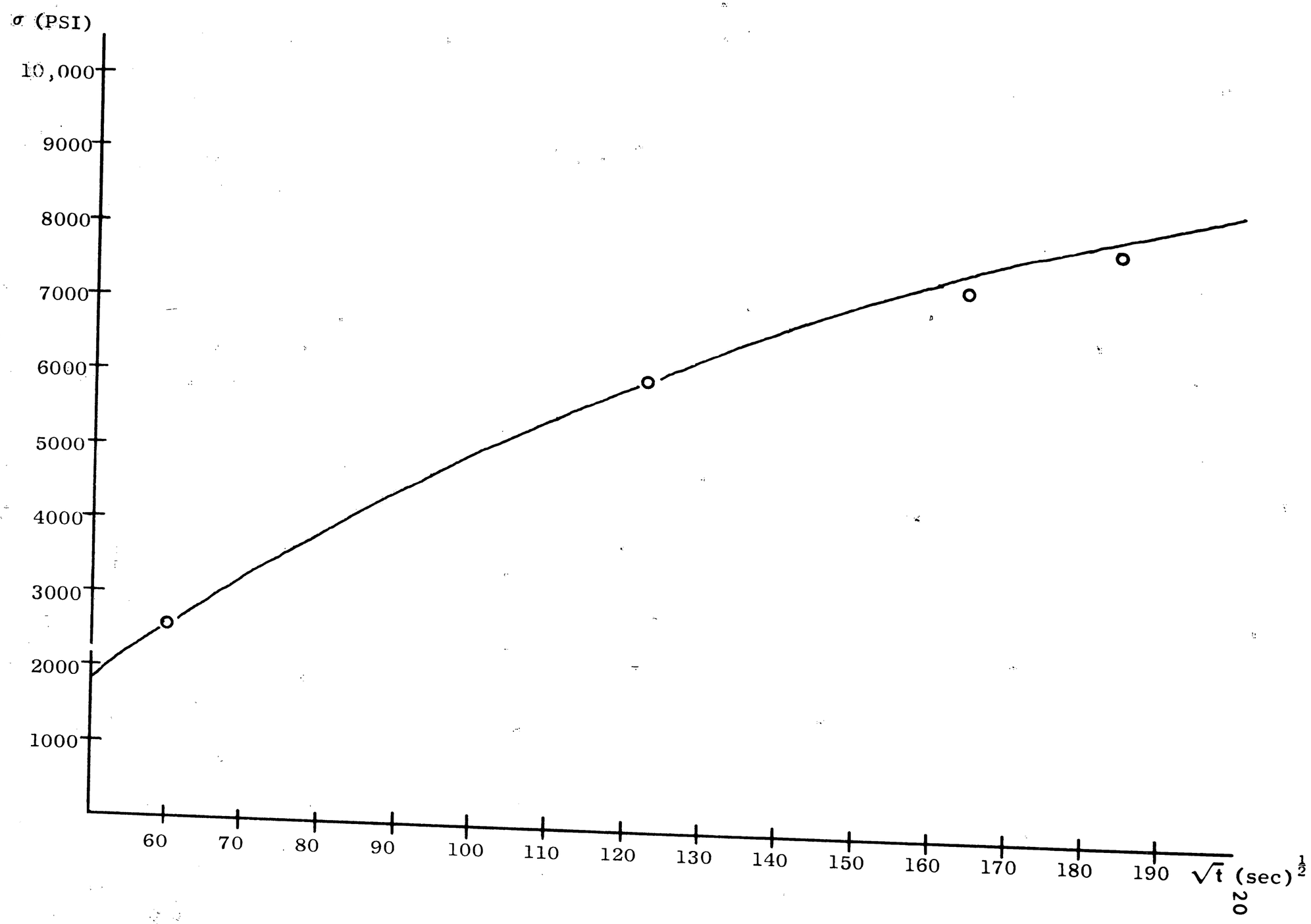

Figure 2
Maximum Tensile Strength vs $\sqrt{t}$ for Specimens Fired at 1100 °C.

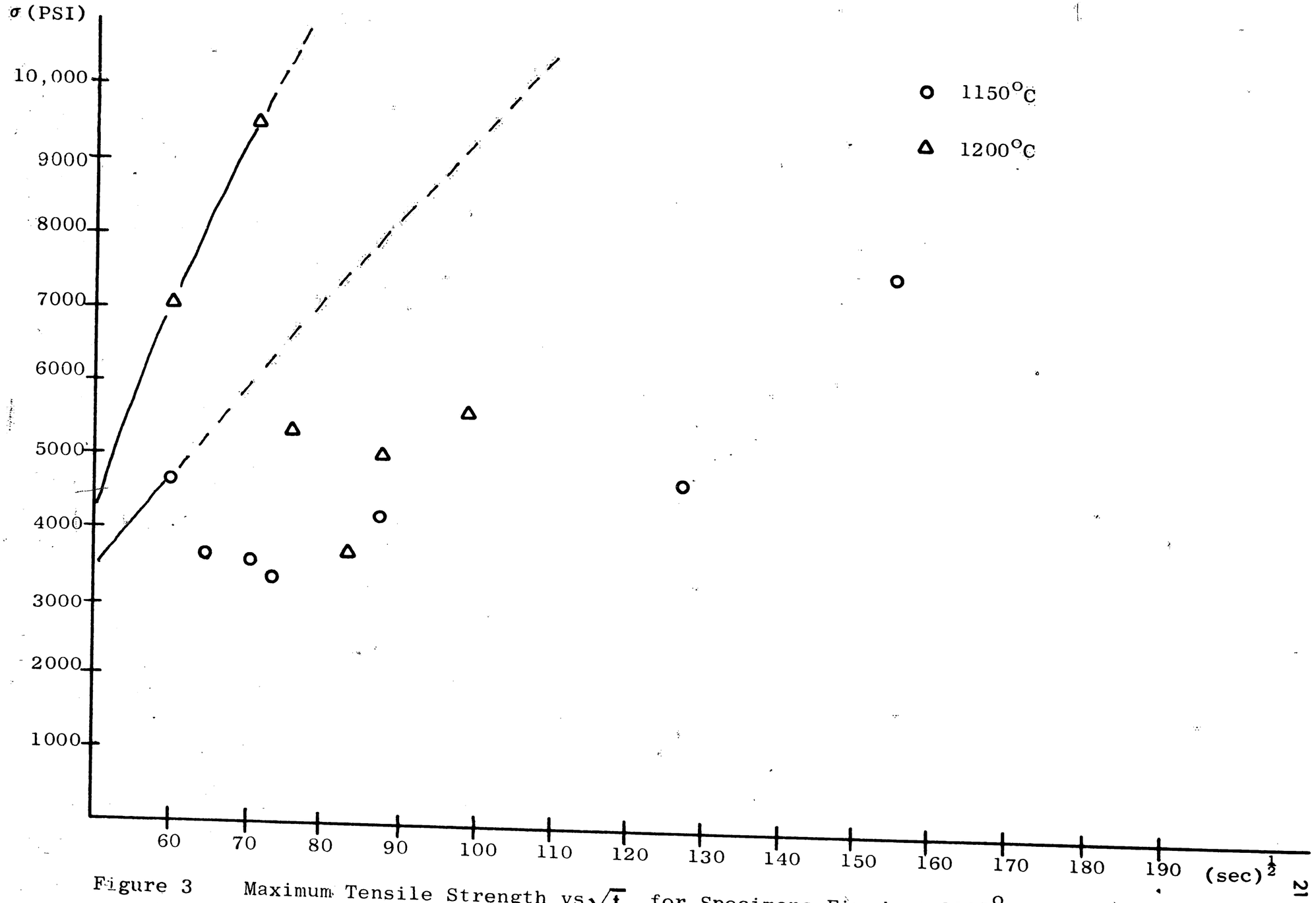

Figure 3 Maximum Tensile Strength vs $\sqrt{t}$ for Specimens Fired at 1150°C and 1200°C.

B. Microscope Observations of Separated Interfaces

Optical and electron photomicrographs of separated interfaces yield much information about the adhesive bond. The most prominent feature in the gold revealed under the microscope are gas occlusions trapped at the interface. Figure 4 is a photomicrograph of a gold drop containing some rather large occlusions that are actually visible to the naked eye. Slip lines are also visible on the surface of the gold.

Very small gas occlusions that are invisible to the naked eye are in the form of negative crystals. Figure 5 is a series of photomicrographs showing some of these negative crystals of various shapes. Figure 5b and 5c show slip lines in the gold while the lines in 5a are replicas of polishing scratches in the sapphire disk. An especially interesting feature in 5c is the grain boundary passing through the center of the picture.

Figure 6 is a series of electron photomicrographs of a surface replica of the gold surface shown in Figure 5a. It is a two stage replica shadowed at 30^{o} with C-Pt. From the shadowing it was determined that the gas occlusions are indeed depressions in the gold surface and the spots spread uniformly over the gold surface are raised. These spots bear a striking resemblence to oxide nuclei seen on iron specimens. The drop in these photographs was fired in oxygen.

The most striking features on the sapphire interface that were revealed under the optical microscope were the gold arcs on portions of the perimeter of the interface as shown in Figure 7a and 7b and gold

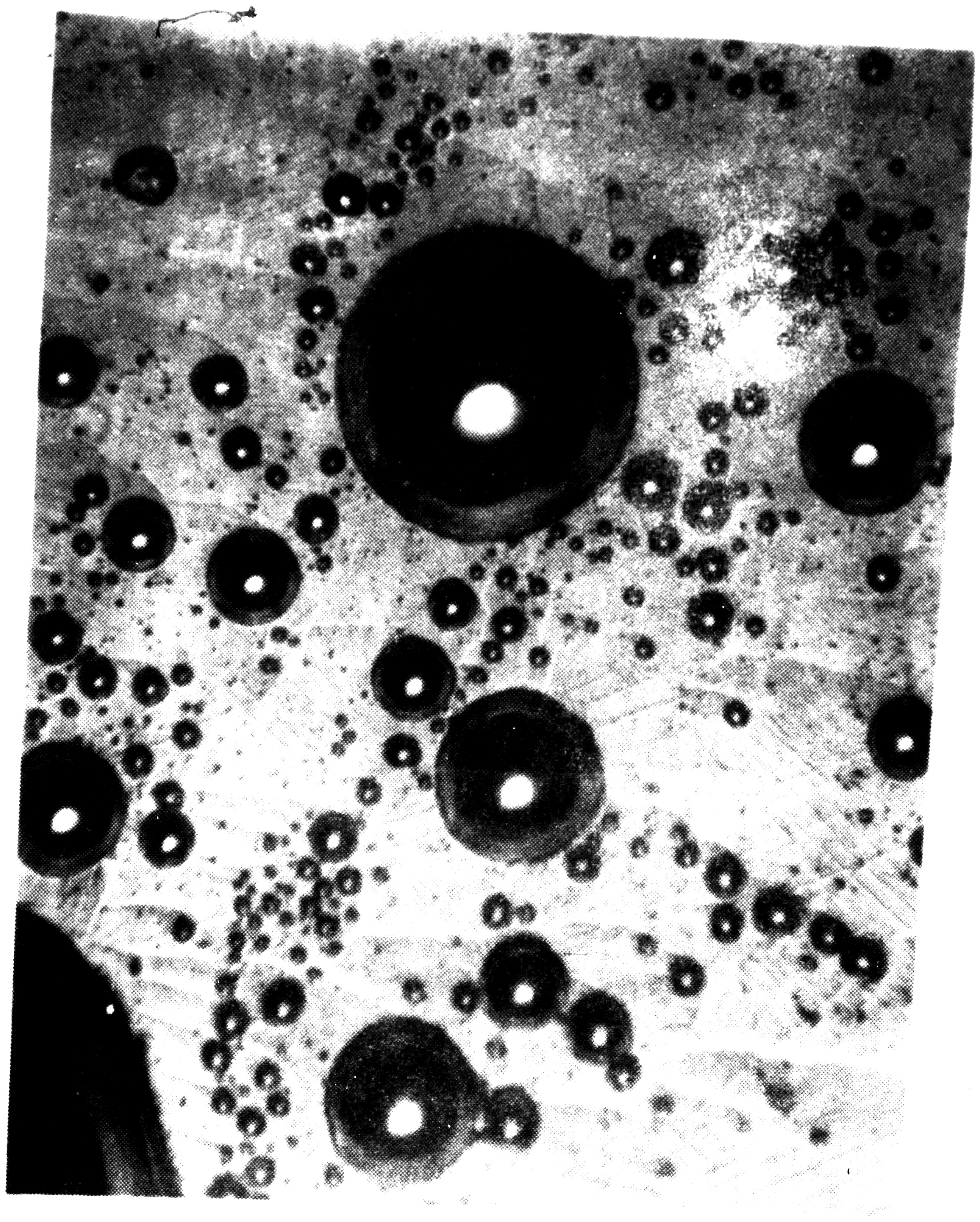

Figure [illegible]
Ga[illegible] Oc[illegible] [illegible] (200X).

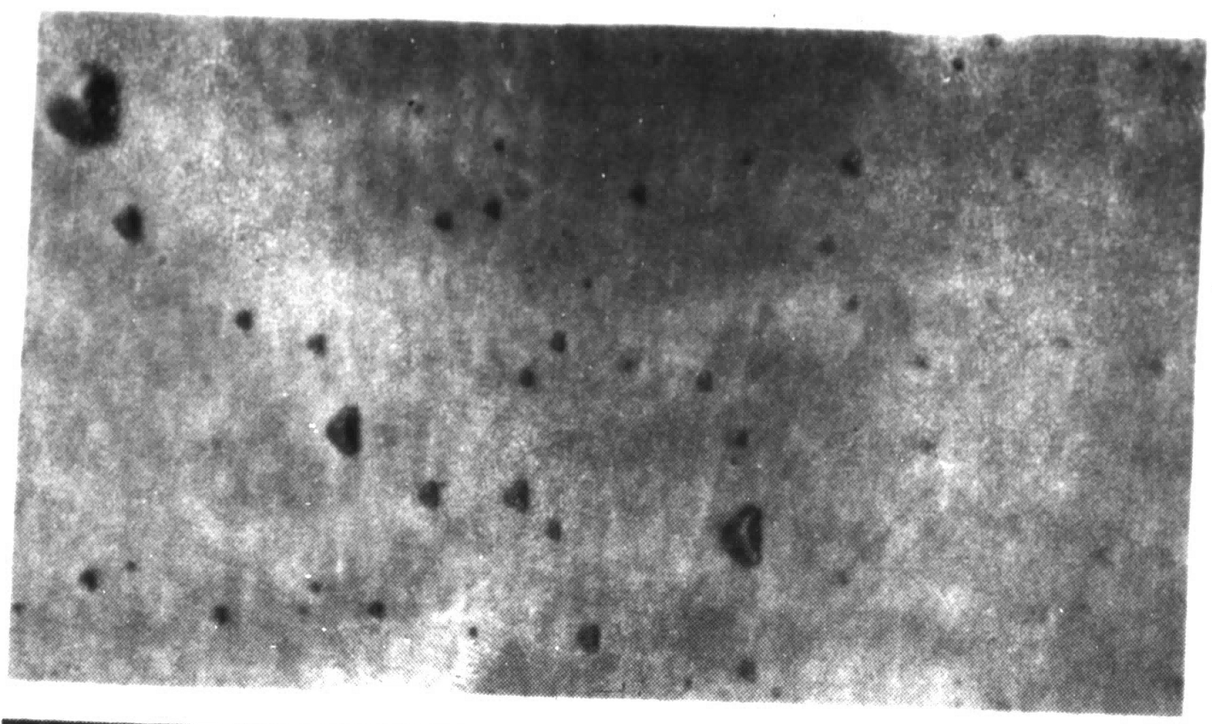

5a
(1000X)

5b
(500X)

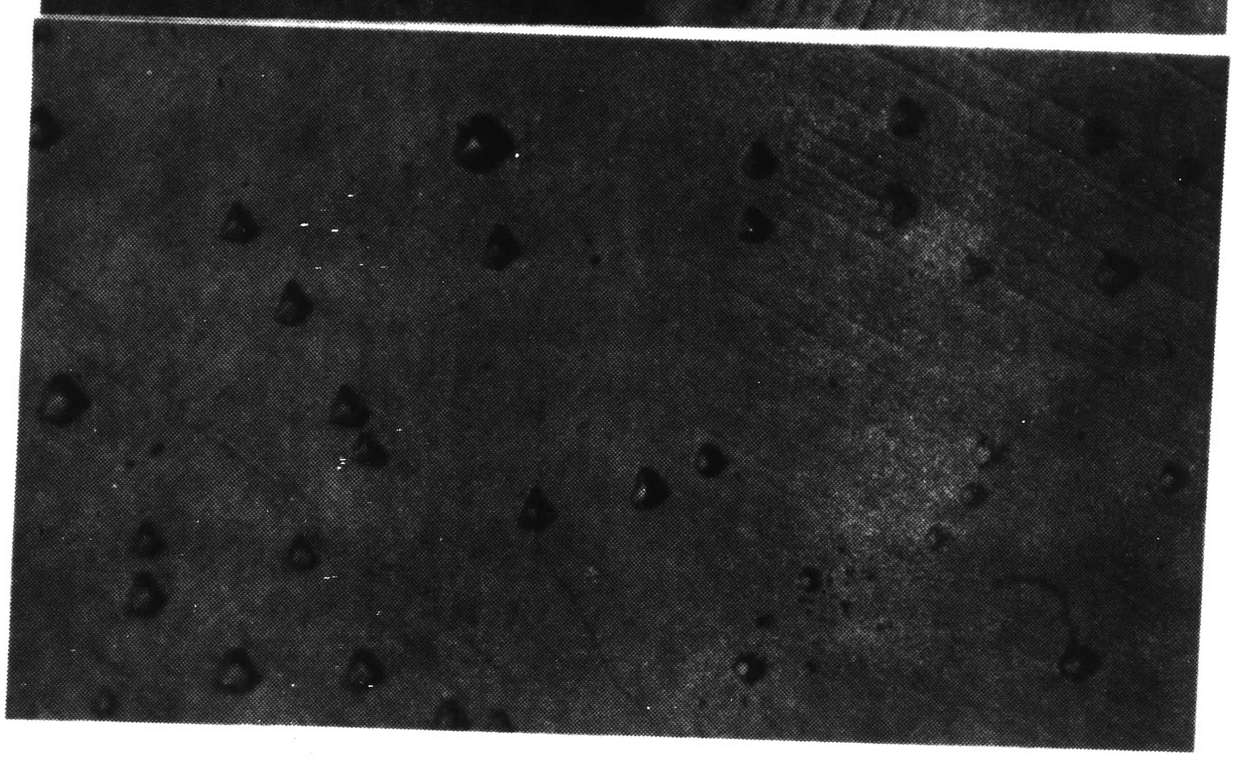

5c
(500X)

Figure 5
Microscopic Gas Occlusions in a Gold Drop.

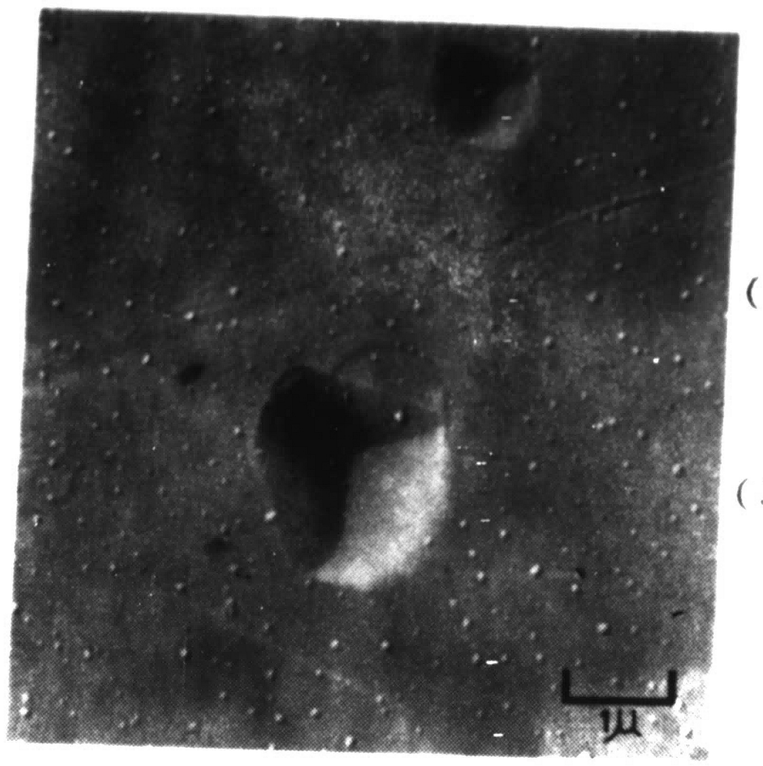

6a
(10,000X)

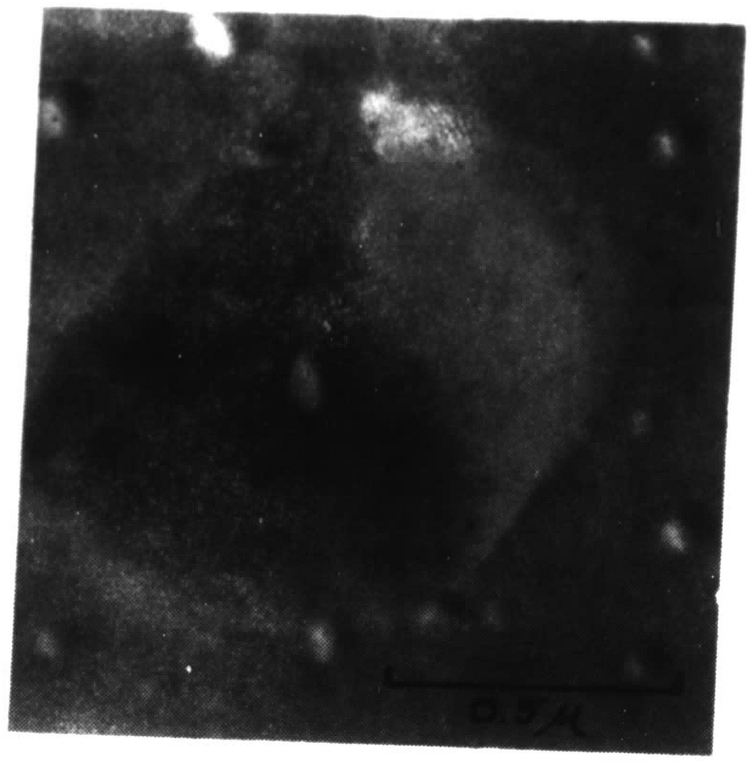

6b
(50,000X)

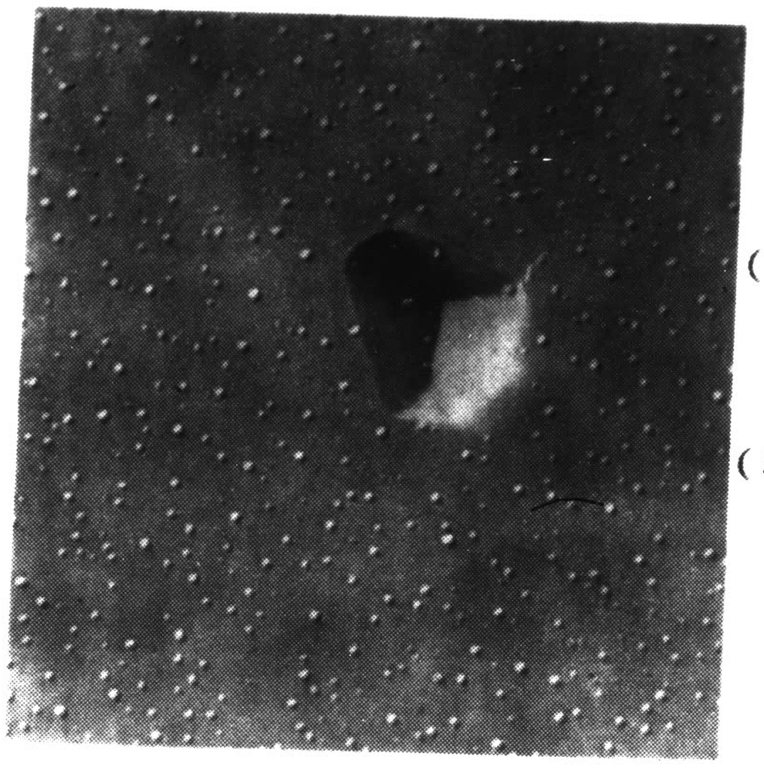

6c
(10,000X)

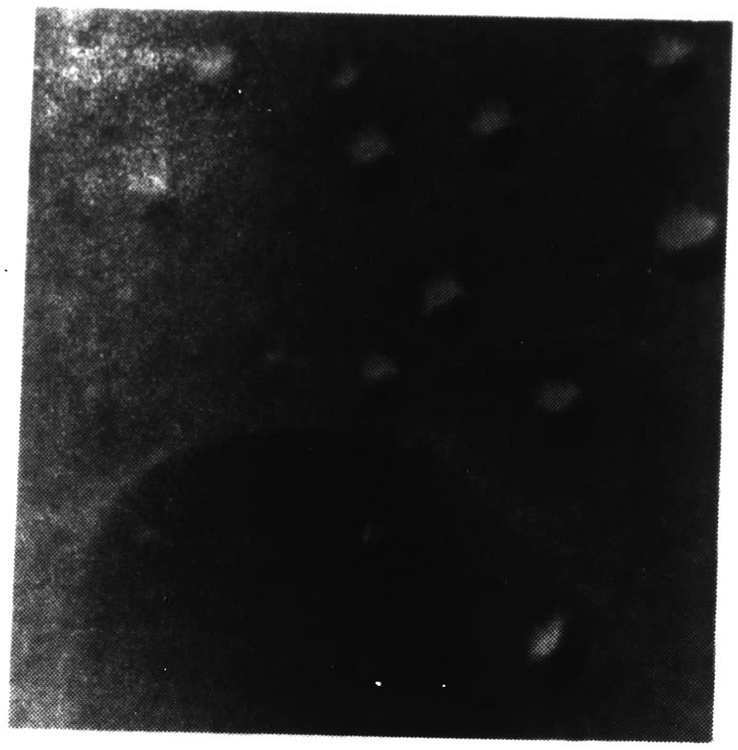

6d
(50,000X)

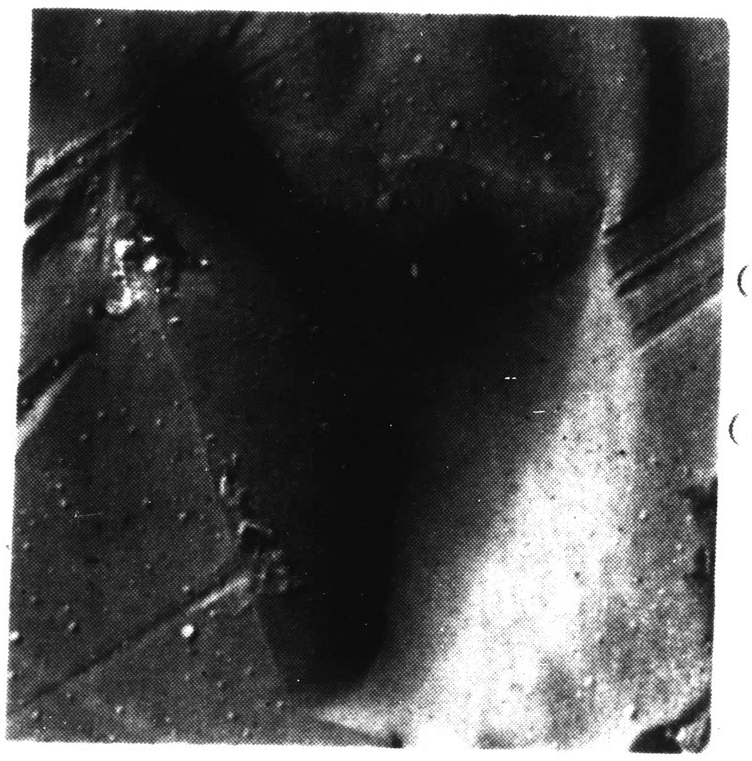

6e
(10,000X)

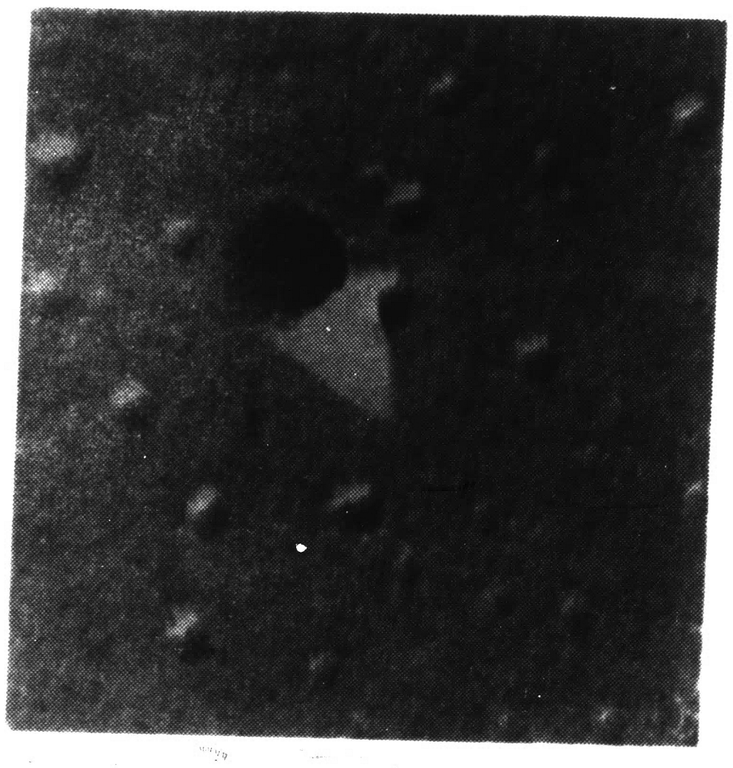

6f
(50,000X)

Figure 6

Electron Photomicrographs of the Gas Occlusions Shown in Figure 5a.

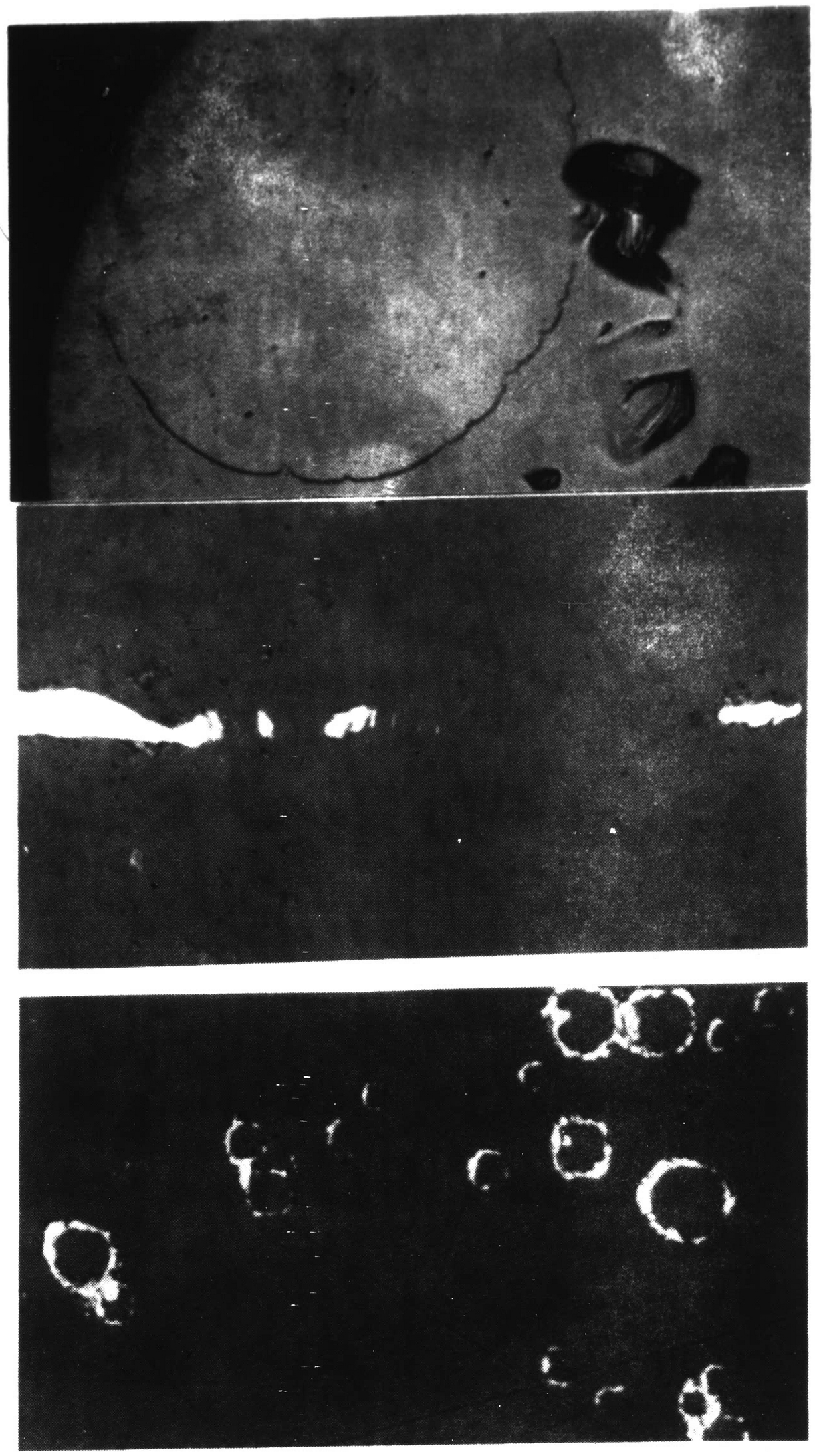

7a
(25X)

7b
(500X)

7c
(500X)

Figure 7
Gold Remaining on Sapphire Surface After Pull Test.

circles around the perimeters of gas occlusions of specimens fired in oxygen and nitrogen as shown in Figure 7c. Figure 7a is a low magnification photograph of a gold arc that covers nearly the whole perimeter of the interface. The dark areas are sapphire pullouts from previous tests. Figure 7b is a high magnification photograph of a portion of a gold arc on the perimeter of the interface. It is discontinuous because part of it has been scraped away to show that the sapphire underneath has not been attacked by the gold, at least not to an extent visible at this magnification. Thus, the gold arcs are not filled etch pits. The specks on the sapphire are spots of a contaminating substance, apparently from the interior of the furnace. Analysis of this substance by optical emission spectroscopy employing a laser microprobe showed that it is composed of iron, titanium, magnesium, and zirconium.

Figure 7c is a photomicrograph of gold circles removed from the perimeters of gas occlusions. Polishing scratches can be seen on the sapphire surface.

It is presumed that the gold drops are usually single crystals underneath their curved surfaces. There are at least two indications of this. First, the negative crystals, when they appear, usually have the same orientation across the interface. An exception is shown in Figure 5c. Second, when a gold drop is etched in aqua regia its cubic symmetry becomes apparent after a short while. Figure 8 is a pair of photomicrographs of two etched gold drops on a sapphire disk. The smaller one is oriented with its (111) planes parallel to the interface. Back reflection Laue photographs of either the flat interface portion or the curved surface portion of the gold drops do not reveal the pattern

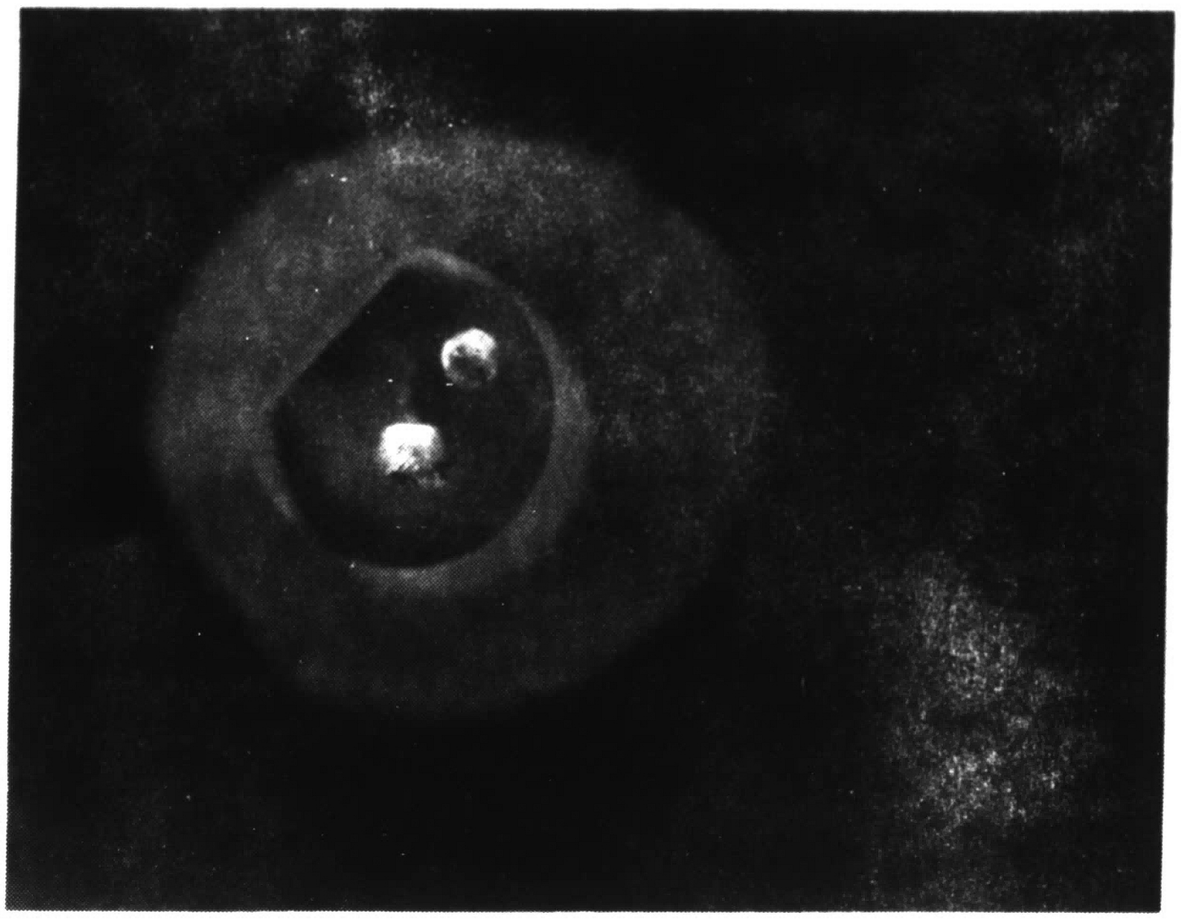

8a
(4X)

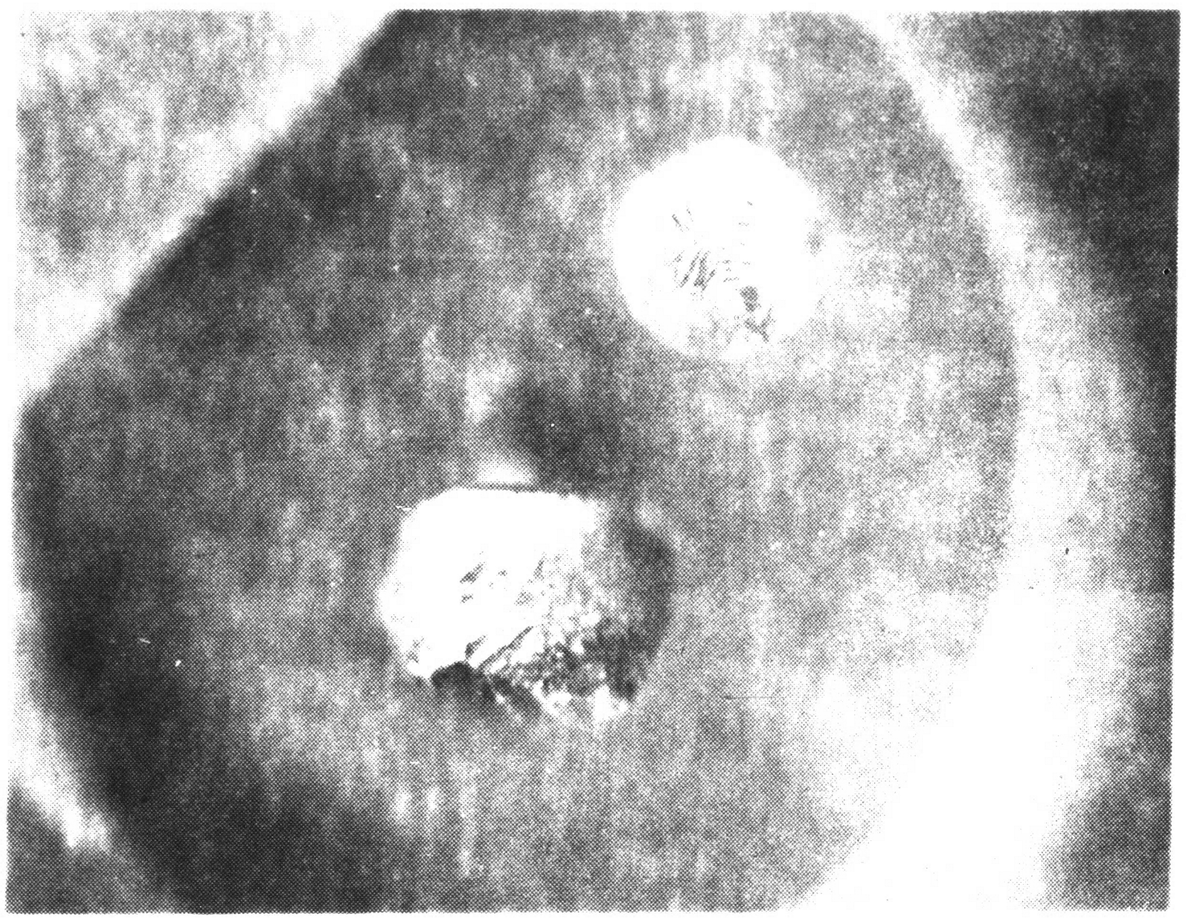

8b
(15X)

Figure 8
Etched Gold Droplet on a Sapphire Disc

characteristics of a single crystal. This is believed to be due to the fact that the gold near the interface has been distorted by rotating slip planes and the curved surface is not part of the single crystal. If the drops were either etched or polished before taking the Laue photograph, the pattern of a single crystal should become evident.

Features revealed on the sapphire interface by the electron microscope are shown in the next figure. Figure 9 is a series of photomicrographs of a surface replica of the sapphire interface after separation. It is a two stage replica shadowed at 30^{o} with C-Pt.

Figure 9a and 9b are pictures of a region of the sapphire surface containing a portion of the perimeter of what was the interface. The area with the parallel polishing scratches is outside the interface. The perimeter itself is characterized by sapphire pullouts and a contaminating substance. The interior of the interface has a wavy appearance. There are three possibilities for the origin of this wavy appearance:

(1) The surface observed may not be sapphire, but gold left behind when the interface was separated.

(2) The surface may have been chemically attacked by the gold.

(3) The sapphire may have been plasitcally deformed when the interface was separated.

However, since the pull test was performed at room temperature it does not seem likely that the sapphire plastically deformed. The tensile stress required to separate this specimen was 5380 lb/in^2.

The possibility that the surface is really a thin layer of gold

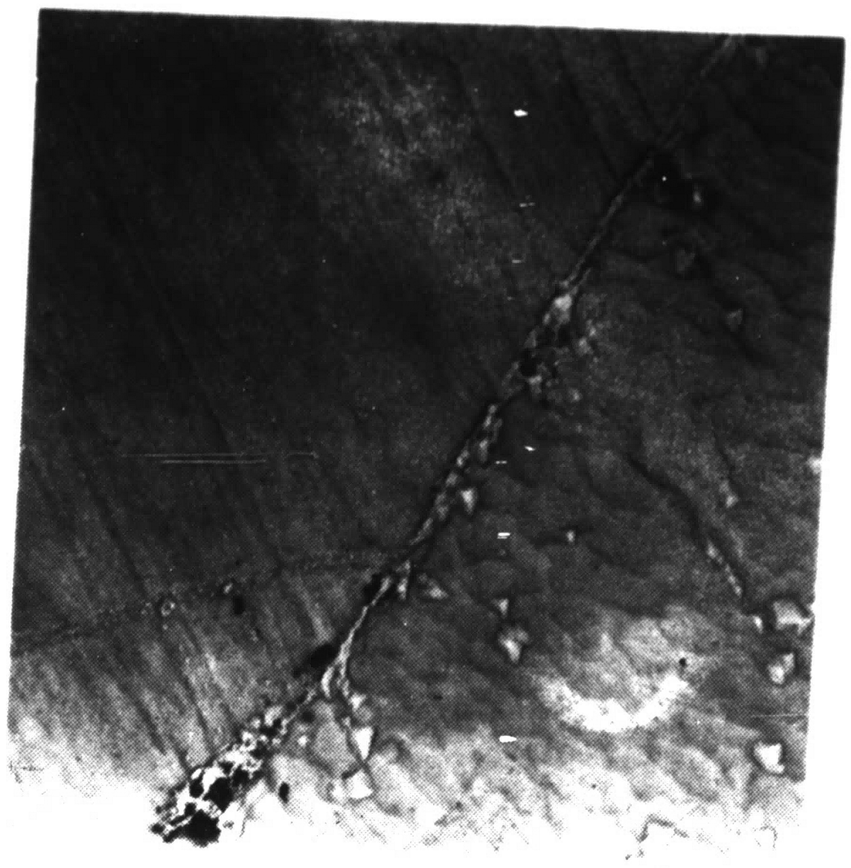

9a
(2400X)

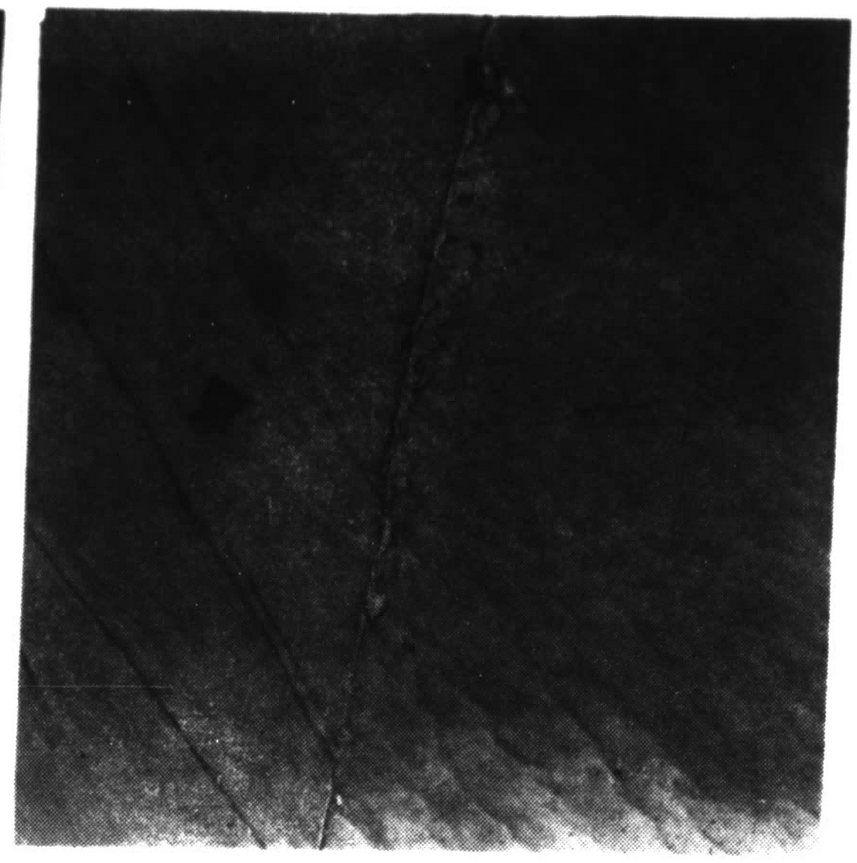

9b
(2400X)

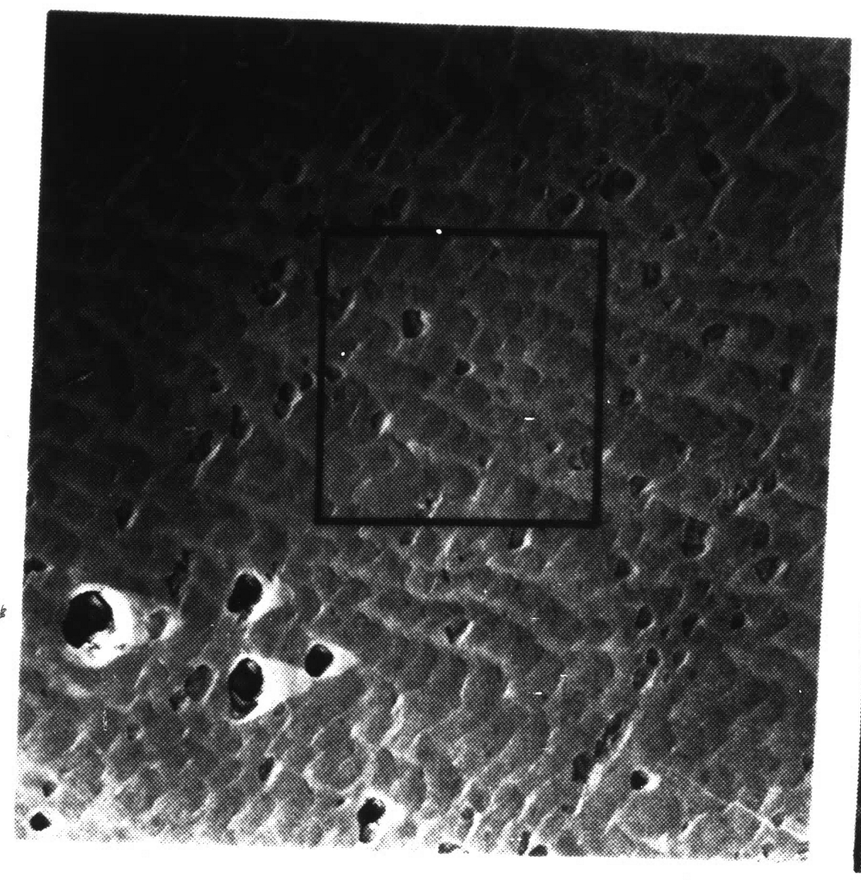

9c
(2400X)

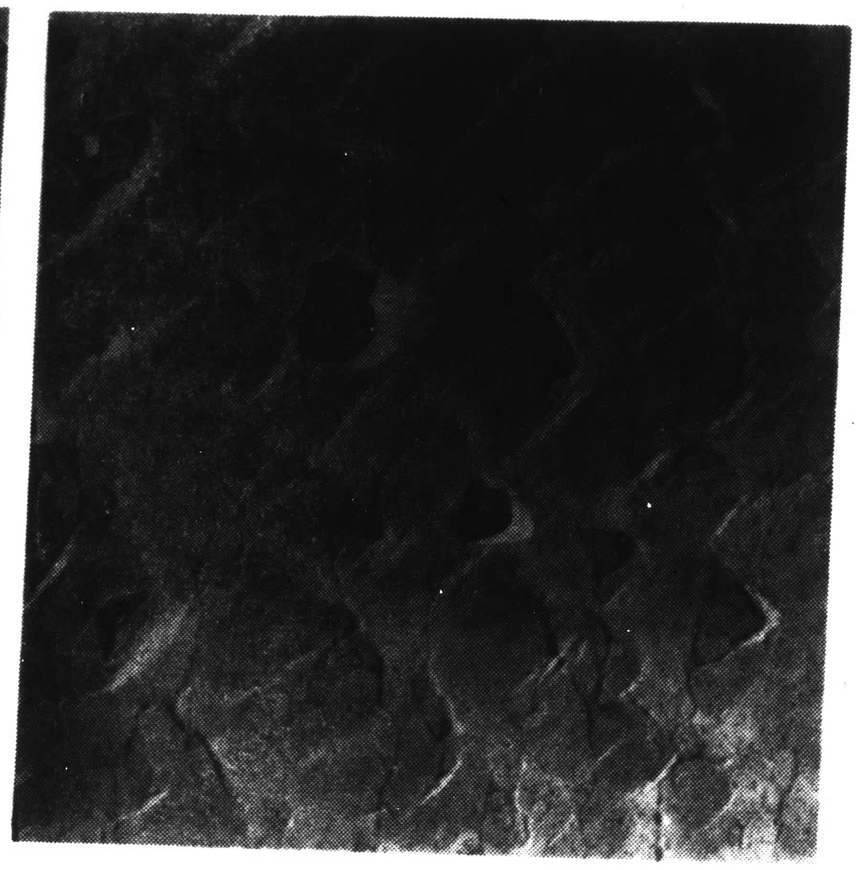

9d
(10,000X)

Figure 9
Electron Photographs of Sapphire Interface.

does not seem likely either. There was no evidence of gold on the interface under an optical microscope.

The most likely explanation is that the sapphire surface has been chemically attacked. It should be noted that this does not necessarily imply that chemical bonds were formed.

The pyramid shaped spots in Figure 9a are sapphire pullouts. The black specks in the photographs are due to defects in the photographic plates.

Figures 9c and 9d are photomicrographs of an area of the sapphire surface in the interior of the interface. Figure 9d is an enlargement of the portion outlined in Figure 9c. The dark spots are sapphire pullouts as indicated by their shadows.

Figures 10a and 10b are photomicrographs of a portion of what was the interface on the gold drop. Figure 10b is a blow up of the area marked in Figure 10a. There are several features of interest in these last two photographs. The geometric shapes in these pictures are gas occlusions. Slip lines are evident in Figure 10a. The surface of the gold appears to be covered with microcracks. The small dark spots in Figure 10b might be oxide nuclei although they are smaller than those seen in Figure 6. This specimen was also fired in an oxygen atmosphere.

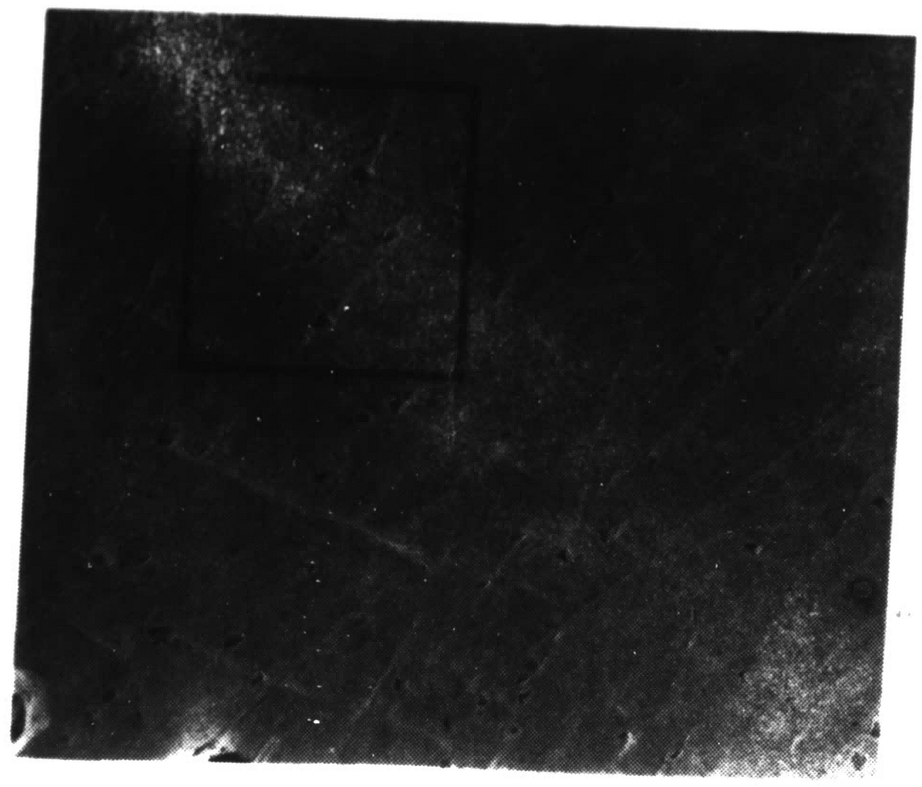

10a
(2400X)

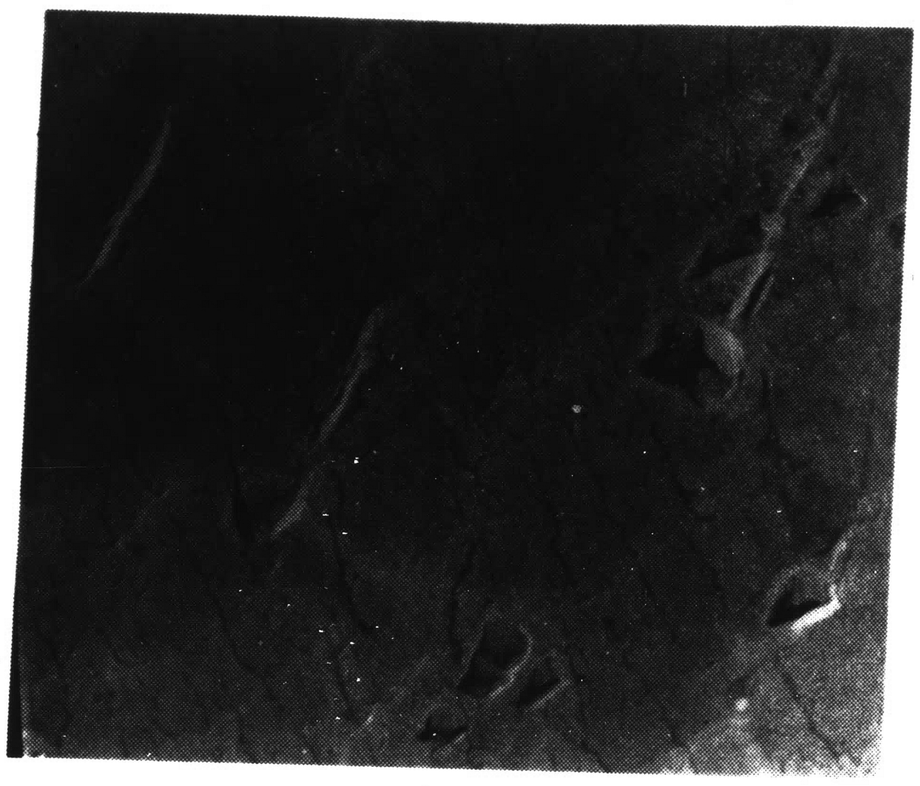

10b
(10,000X)

Figure 10
Electron Photomicrographs of Gold Interface.

V. DISCUSSION

It is the purpose of this section to develop a bonding model for the gold/sapphire system which is sufficient to explain the experimental results.

In Appendix II the Young-Dupre equation, which relates the contact angle of a liquid drop to a solid surface, is derived:

(1) $W_{AD} = {}_{l}\gamma_{v}\{1 + \cos\theta\}$ where

W_{AD} is the work of adhesion

${}_{l}\gamma_{v}$ is the surface tension of the liquid in equilibrium with its vapor

θ is the equilibrium contact angle

This equation is valid so long as equilibrium has been reached and no mixing of the solid and liquid occurs.

The Young-Dupre equation also applies to a solid drop in equilibrium with a solid surface provided that no stresses are supported at the interface. However, since the solid drop would have to plastically deform to change its contact angle, the contact angle measured at room temperature is probably the contact angle that satisifies the Young-Dupre equation at the freezing point of the liquid. If this is taken to be the case, the expected contact angle of gold on sapphire can be calculated from the appropriate data at 1063°C. Equation (1) can be rearranged to give

$$(2) \quad \theta = \cos^{-1}\left\{\frac{W_{AD}}{{}_{l}\gamma_{v}} - 1\right\}$$

In Appendix I it is shown that the work of adhesion is nearly independent of temperature for any system bound only by van der Waals dispersion forces.* The derivation of the Young-Dupre equation in Appendix II was independent of ambient atmosphere, i.e., it applies in any atmosphere and can be used numerically as long as the surface tension of the liquid is measured under the same conditions as the contact angle. If the bonds in the gold/sapphire system are assumed to be of the dispersion type and the surface tension of gold measured in air is the same as that measured in oxygen, the value of W_{AD} measured by Pilliar and Nutting[50] and the value of γ_v given by Bondi[3] can be used in equation (2) to calculate the equilibrium contact angle for gold melted on sapphire in oxygen.

$$(3)\quad \theta = \mathrm{Cos}^{-1}\left\{\frac{530}{1134} - 1\right\} = \mathrm{Cos}^{-1}\{-.532\} = 122.1^{o}$$

Since the measured contact angles are very near to this value, it is evident that at least the perimeters of the interfaces have reached equilibrium, or nearly so, in the course of the experimental runs.

The photomicrographs in Figure 7 indicate that the bond between the gold and the sapphire near the perimeter of the interface had a tensile strength of at least the tensile strength of gold. Since the tensile strength of gold is about 30,000 PSI, it is evident that at or near equilibrium bonds between gold and sapphire will support very high

---

* r, N_c, and N_m are slightly temperature dependent.

tensile stresses and that the system as a whole had not reached equilibrium in the course of the experimental run. This fact and the fact that the tensile strength of the bonds increases with time at a temperature dependent rate form the basis for formulating a bonding model for the gold/sapphire system.

Consider an ideal system consisting of a solid piece of gold resting on a polished sapphire disk at 25 ^{o}C and one atmosphere pressure in a one component atmosphere. Both the gold and the sapphire have been cleaned so that their surfaces are free of gross contaminants. They will have, however, a layer of adsorbed gas on them, either physically adsorbed or chemisorbed or both. The composition of this adsorbed layer is going to depend upon the previous history of the gold and sapphire as well as the composition of the ambient atmosphere. As the temperatures is raised, these miscellaneous adsorbed gases are gradually replaced by an adsorbed layer of the ambient atmosphere, the rate at which this takes place being dependent upon the nature of the adsorbed gases and the temperature. At temperatures approaching 1000 ^{o}C the replacement should be extremely rapid and the adsorbed layer is essentially of the same species as the ambient atmosphere. When the gold melts at 1063 ^{o}C, it assumes the shape of a sessile drop. The liquid gold and sapphire at this point are separated by a layer of adsorbed gas. If it is assumed that no chemical bonds form between gold and sapphire, the only forces of attraction of any consequence between them are London's dispersion forces acting across the gap that separates the gold and the sapphire. Since these forces decrease rapidly with separation, the adhesive forces will be relatively small,

their exact magnitude being dependent only on the thickness of the intervening layer. Thus, the tensile strength of the gold/sapphire bond could be calculated if the thickness of the intervening layer were known. It should be noted that this only applies to systems which do not develop stresses at the interface on cooling. It has been shown by Moore and Thornton[49] that gold does not support such stresses under these conditions.

In most atmospheres, the process of bond formation described above would be a complete description of the bond formation mechanism when gold is melted on sapphire. In the special case where the furnace atmosphere is oxygen, however, the above process is only the first step in the formation of the bond. It is proposed that the important difference between melting gold on sapphire in oxygen and melting it in nitrogen, forming gas, or noble gases is that oxygen reacts with gold chemically to form a layer of gold oxide on the drop which in turn has an adsorbed oxygen layer, thus beginning a series of reactions which result in the gradual reduction of the thickness of the contaminating layer between the gold and the sapphire. In the proposed model the situation at the end of the first step is pictured schematically in Figure 11.

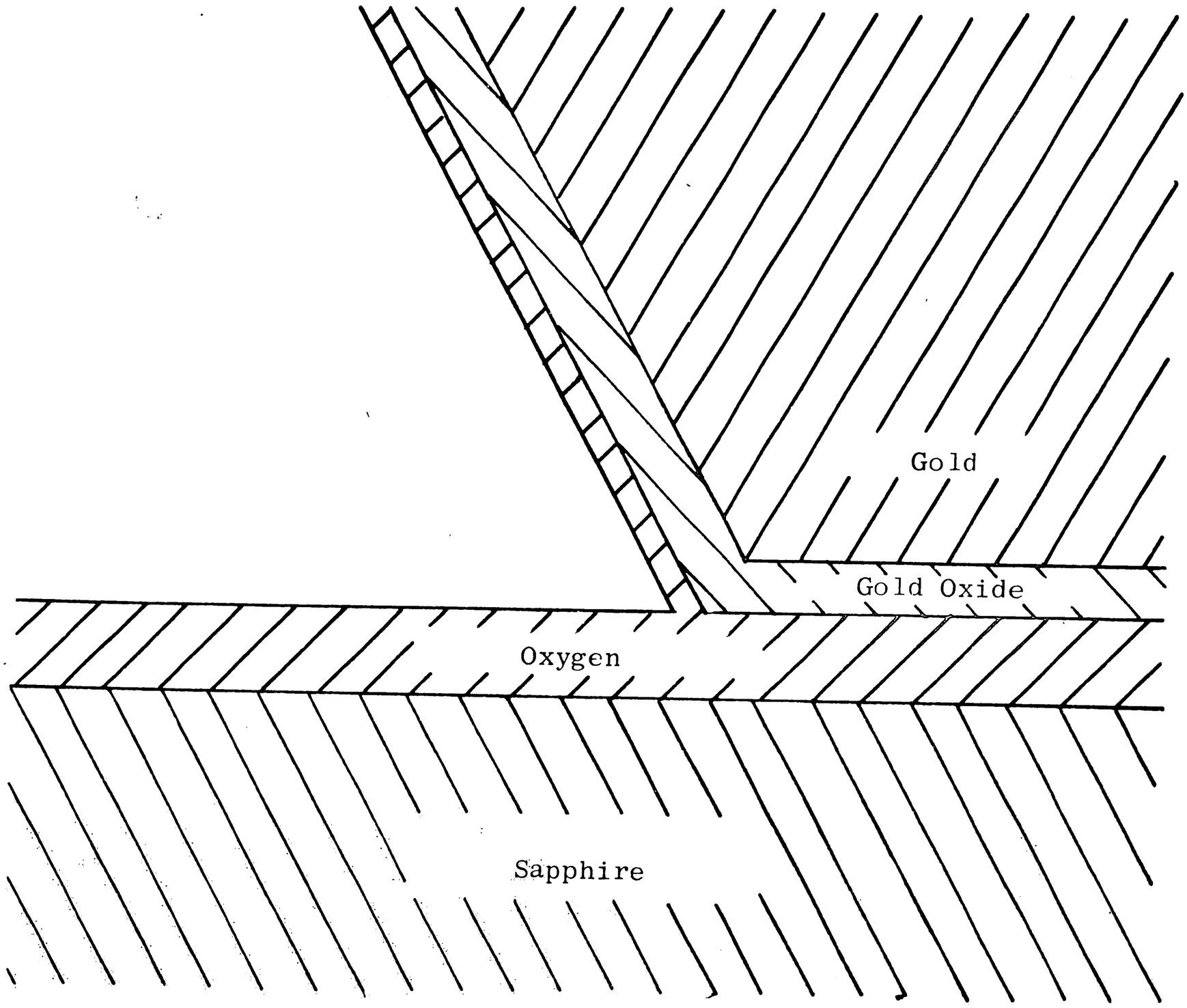

FIGURE 11 The State of a Sessile Drop of Gold on Sapphire in Oxygen at the End of Step One.

It is further proposed that the gold oxide has a relatively high vapor pressure and is constantly escaping from the surface of the gold drop only to be rplaced immediately by more gold oxide. The results of an investigation by Carpenter and Mair[51] support these proposals.

It is postulated that in the immediate neighborhood of the three phase interface, i.e., the perimeter of the gold/sapphire two phase interface, the mechanism of replacement of the lost gold oxide is different than for the rest of the surface of the gold drop. Over most of the surface of the drop the gold oxide is replaced by oxidation of

gold by oxygen from the atmosphere. However, as gold oxide evaporates from the surface of the drop near the three phase interface, it is replaced by oxidation of gold by oxygen from underneath the drop. Since the oxygen density is much higher on the surface of the sapphire than in the ambient atmosphere, this replacement mechanism predominates for some distance from the interface perimeter. This action results in a depletion of the oxygen layer under the gold drop. When all of the uncombined oxygen has been removed from under the gold, step two in the formation of the bond has been completed. The situation aspostulated at the end of step two is shown schematically in Figure 12.

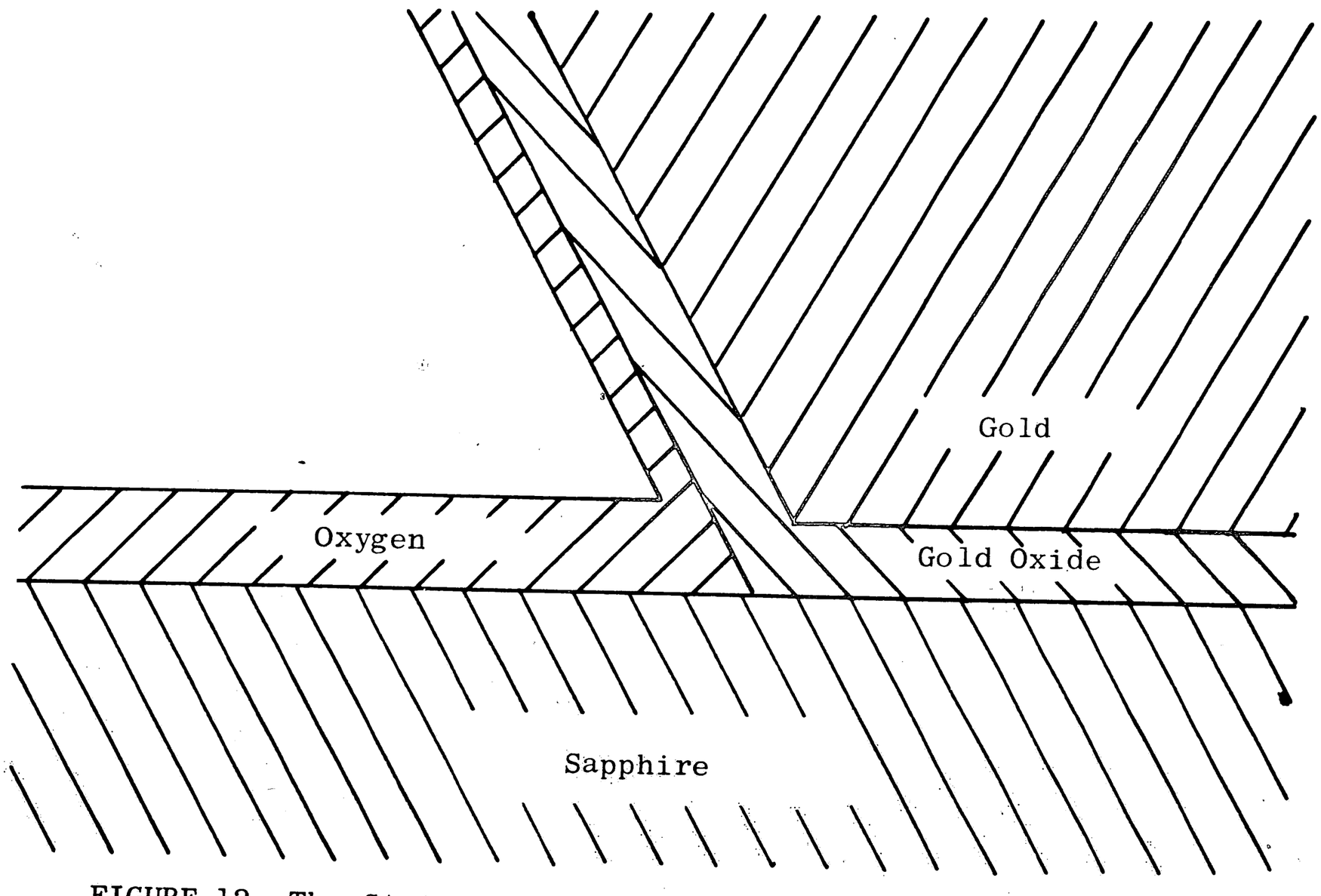

FIGURE 12 The State of a Sessile Drop of Gold on Sapphire in Oxygen at the End of Step Two.

The gold oxide layer enclosing the gold is probably non-stoichiometric and amorphous. It is assumed that this gold oxide layer can support no tensile stresses so that the tensile strength of the bond is due entirely to the dispersion forces acting between the gold and the sapphire.

It seems likely that steps one and two are completed within a few seconds of the time when the gold melts. If the system is then held for a period of time at some temperature, the third step in the process of bond formation becomes operative, the diffusion of gold oxide into the sapphire substrate. By this diffusion the thickness of the gold oxide layer decreases and thus the attractive dispersion forces between the gold and sapphire increase.

Consider the forces acting at the perimeter of the two phase interface shown schematically in Figure 13.

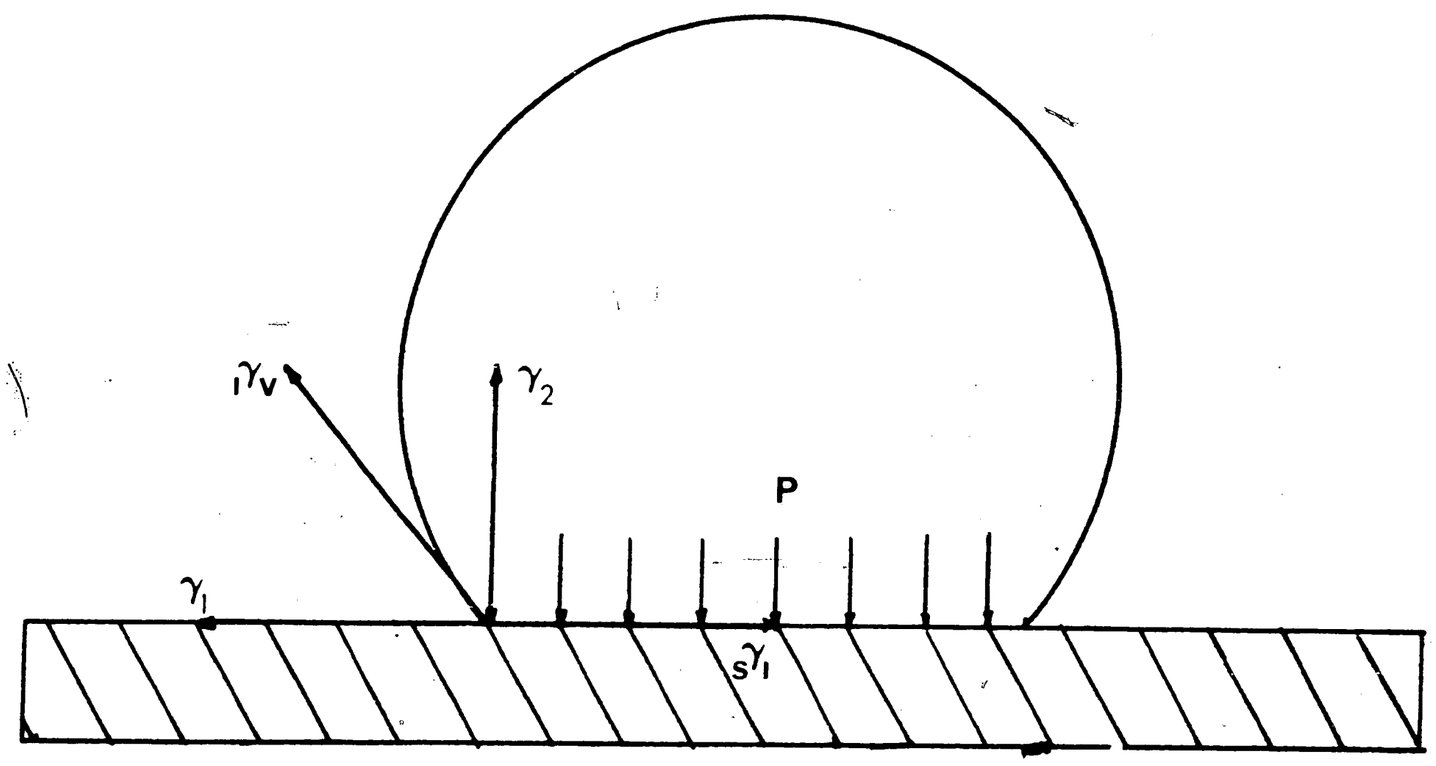

FIGURE 13 Forces Acting on the Perimeter of the Two Phase Interface.

$$\gamma_1 = {}_s\gamma_v + {}_l\gamma_v \cos\theta$$

$$\gamma_2 = {}_l\gamma_v \sin\theta$$

The forces acting parallel to the interface are considered in the derivation of the Young-Dupre equation in Appendix II. The forces acting perpendicular to the interface are of interest here. The force γ_2 is not balanced by a corresponding force acting at the perimeter of the interface but by a force P distributed over the entire interface. This results in the sapphire in the neighborhood of the perimeter of the interface being in tension while the sapphire under the rest of the interface is in compression. It can be shown that the diffusion coefficient increases when the pressure on a body is decreased,[52] hence, the diffusion of gold oxide into sapphire will be faster near the perimeter of the two phase interface than over the rest of the interfacial area. Thus, in the early stages of diffusion of the gold oxide into the sapphire, the gold oxide layer is significantly thinner near the perimeter of the interface than elsewhere and the tensile strength of the adhesive bond there is correspondingly higher.

At the conclusion of the third and final step in the process of bond formation in an oxygen atmosphere, all the gold oxide has diffused into the sapphire, equilibrium has been reached, and the ultimate bond has been obtained.

To test this hypothesis an equation must be derived expressing the tensile stress the interface will support in terms of the important parameters of the system. To do this the following information is needed:

(1) The mechanism of the bond and how its strength varies with the separation of the gold and sapphire.

(2) The rate at which gold oxide will diffuse into sapphire at a given temperature.

(3) The manner in which the diffusion rate is linked to the rate of change of the separation between the gold and sapphire.

It is postulated that the only bonds in the system are van der Waals bonds of the dispersion type. A discussion of van der Waals bonds in Appendix I leads to the equation for the stress required to separate a metal from an ionic crystal when the two phases are bound together only by dispersion forces:

$$(4) \qquad \sigma = -\frac{K}{r^3}$$

where

σ is the tensile stress required to break the bond

K is the adhesion constant (see Appendix I)

r is the separation between the metal and the crystal.

It is of interest to know what tensile strengths equation (4) predicts for the gold/sapphire system. From Appendix I

$$K = 6.24 \times 10^{-13} \text{ dyne cm}$$

The maximum tensile strengths possible for a gold/sapphire system are plotted versus separation according to equation (4) and shown in Figure 14.

It therefore is only necessary to know the separation of the gold and sapphire to be able to predict the tensile strength of the bond. To find how the thickness of the gold oxide layer decreases with time it is necessary to find the rate at which it diffuses into the

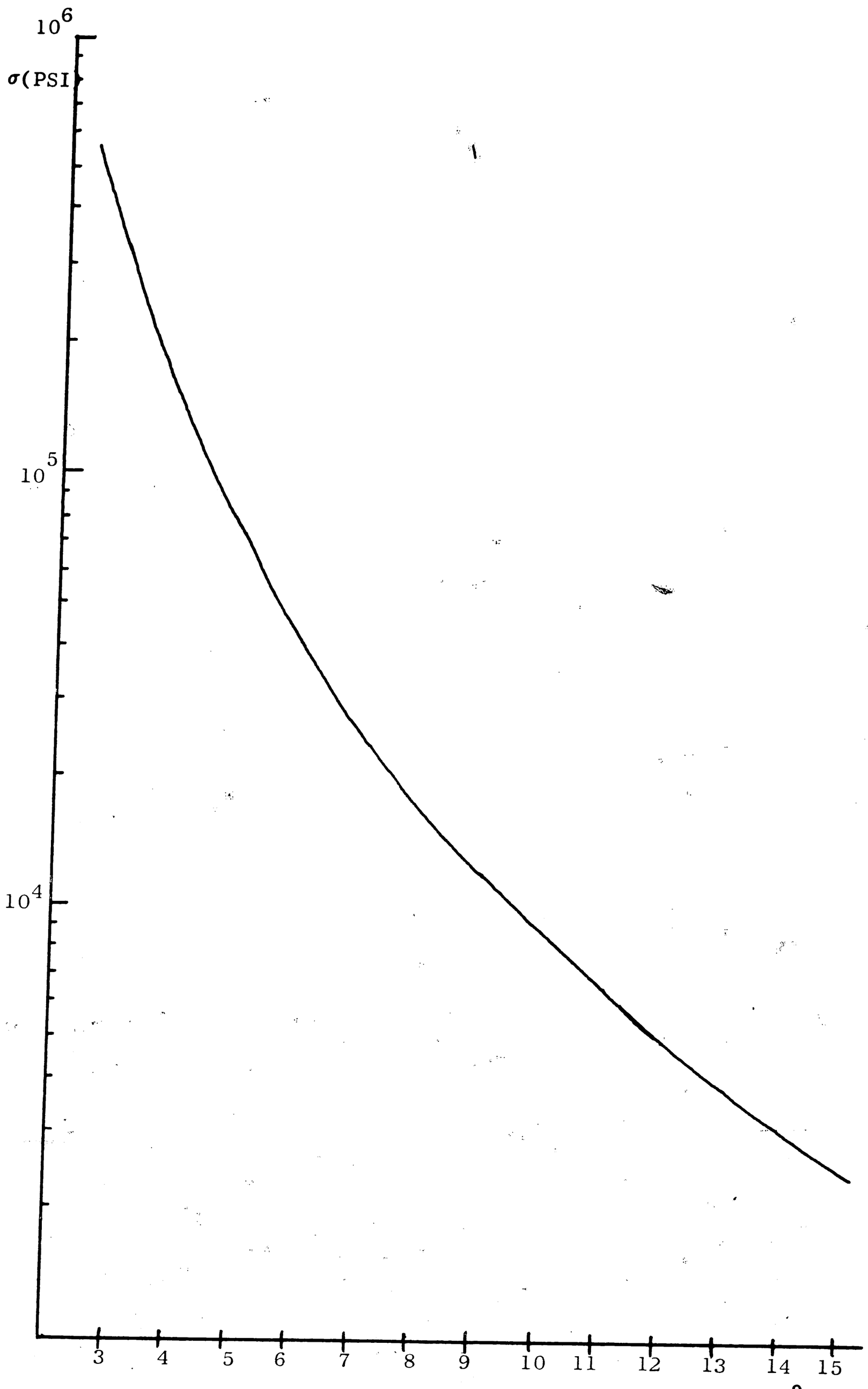

Figure 14 σ vs r

sapphire disk. The gold oxide can be considered to remain at constant concentration between the gold and the sapphire until it has been reduced to a monolayer. Thus the problem is the classic one of solving the diffusion equation when surface of a semi-infinite solid is held at constant concentration. The solution to the differential equation

$$(5) \quad \frac{\partial C}{\partial t} = D \frac{\partial^2 C}{\partial x^2}$$

with the boundary conditions

$$(6) \quad \begin{array}{lll} C = C_o & X = 0 & t \geq 0 \\ C = 0 & X > 0 & t = 0 \end{array}$$

is given by Crank[53] as

$$(7) \quad C = C_o \operatorname{erfc} \frac{x}{2\sqrt{Dt}}$$ where

C is the volume concentration of gold oxide below the sapphire surface.

C_o is the volume concentration of gold oxide on the sapphire surface.

X is the distance below the sapphire surface.

D is the diffusion coefficient.

t is the time the specimens are held at the temperature of interest.

and $\operatorname{erfc} z \equiv 1 - \operatorname{erf} z$

If the initial quanitiy of gold oxide between the gold and the sapphire is M_o units of gold oxide per unit area of interface, then

(8) $M_o = d_o C_o$ where

d_o is the initial thickness of the layer of gold oxide.

The total amount of gold oxide that has diffused into the sapphire per unit area of interface is

$$(9) \quad I(t) = \int_0^\infty C(x,t)\,dx = C_o \int_0^\infty \operatorname{erfc} \frac{x}{2\sqrt{Dt}}\,dx$$

It can be shown that[53]

$$(10) \quad \int_0^\infty \operatorname{erfc} z\,dz = (\pi)^{-\frac{1}{2}}$$

Let $z = \frac{x}{2\sqrt{Dt}}$ $dz = \frac{dx}{2\sqrt{Dt}}$

$$(11) \quad I(t) = 2C_o\sqrt{Dt}\int_0^\infty \operatorname{erfc} \frac{x}{2\sqrt{Dt}}\,\frac{dx}{2\sqrt{Dt}} = \frac{2C_o}{\sqrt{\pi}}\sqrt{Dt}$$

Let the quantity of gold oxide per unit area of interface between the gold and the sapphire at any time t be

(12) $M(t) = C_o\, d(t)$

From the law of conservation of mass

(13) $M(t) + I(t) = M_o$

Substituting (8), (11), and (12) into (13)

$$(14) \quad C_o d(t) + \frac{2C_o}{\sqrt{\pi}}\sqrt{Dt} = d_o C_o$$

This can be rearranged to give

$$(15) \quad d(t) = d_o - \frac{2}{\sqrt{\pi}}\sqrt{Dt}$$

Equation (15) gives the rate at which the contaminating layer is shrinking and is applicable until the contaminating layer has been reduced to a monolayer.

When the gold oxide has been reduced to a monolayer, the boundary conditions on the diffusion equation change. The problem is now one of solving the diffusion equation for a layer of finite thickness on the surface of a semi-infinite crystal. The solution of the diffusion equation with the boundary conditions

$$(16)\quad \begin{aligned} C &= C_o \quad x < h \quad t = 0 \\ C &= 0 \quad x > h \quad t = 0 \end{aligned}$$

is given by Crank[53] as

$$(17)\quad C = \frac{1}{2} C_o \left\{ \operatorname{erf} \frac{h - x}{2\sqrt{Dt}} + \operatorname{erf} \frac{h + x}{2\sqrt{Dt}} \right\}$$

where

h is the thickness of a monolayer

At the surface X = 0 and equation (18) becomes

$$(18)\quad C(0,t) = C_o \operatorname{erf} \frac{h}{2\sqrt{Dt}}$$

Let the surface concentration of the partial monolayer of gold oxide be M'.

Then

$$(19)\quad M'(t) = hC(0,t) = hC_o \operatorname{erf} \frac{h}{2\sqrt{Dt}}$$

where

t = 0 is the time at which the gold oxide becomes a monolayer

In order to be able to use the same time base as before the gold oxide became a monolayer, a new time variable is defined,

(20) $t' = t - t_1$ where

t_1 is the time after diffusion begins that the gold oxide becomes a monolayer

Equation (19) becomes

(21) $M'(t') = hC_o \operatorname{erf} \frac{h}{2\sqrt{Dt'}}$ or

(21a) $M''(t) = hC_o \operatorname{erf} \frac{h}{2\sqrt{D(t-t_1)}}$

(22) $M''(t_1) = M_o'' = hC_o$

Substitute equation (22) into (21a)

(23) $M''(t) = M_o'' \operatorname{erf} \frac{h}{2\sqrt{D(t-t_1)}}$

The stress required to separate the gold and the sapphire at $t > t_1$ is given by

(24) $\sigma = \sigma_1 + \sigma_2$ where

(25) $\sigma_1 = -\frac{K}{r_1^3} X_1$

(26) $\sigma_2 = -\frac{K}{r_2^3} X_2$ where

(27) $r_1 = r_o + h$

(28) $r_2 = r_m$ (see Appendix I for definition of terms)

(29) $X_1 = 1 - \frac{M''(t)}{M_o''} = \operatorname{erfc} \frac{h}{2\sqrt{D(t-t_1)}}$

(30) $X_2 = \frac{M''(t)}{M_o''} = \operatorname{erf} \frac{h}{2\sqrt{D(t-t_1)}}$

Substituting (25), (26), (27), (28), (29), and (30) into (24) gives

$$(31)\quad \sigma = -K\left\{\frac{1}{\{r_o+h\}^3}\,\mathrm{erfc}\frac{h}{2\sqrt{D(t-t_1)}} + \frac{1}{r_m^3}\,\mathrm{erf}\frac{h}{2\sqrt{D(t-t_1)}}\right\} \quad \text{when } t>t_1$$

$$(32)\quad r = r_o + d(t) = r_o + d_o - \frac{2}{\sqrt{\pi}}\sqrt{Dt} \quad \text{when } t<t_1$$

Substituting equation (32) into (4)

$$(33)\quad \sigma = -\frac{K}{\left\{r_o+d_o-\frac{2}{\sqrt{\pi}}\sqrt{Dt}\right\}^3} \quad \text{when } t<t_1$$

Equations (31) and (33) give the tensile strength of the bond as a function of time and temperature since

$$(34)\quad D = D_o e^{-Q/RT}$$

Equations (31) and (33) contain three unknown quantities, D, h, and d_o. These unknowns can be evaluated from the experimental data.

$$(35)\quad \sigma_m = -\frac{K}{r_m^3}$$

Divide equation (35) by equation (33)

$$(36)\quad \frac{\sigma_m}{\sigma} = \frac{\left\{r_o+d_o-\frac{2}{\sqrt{\pi}}\sqrt{Dt}\right\}^3}{r_m^3}$$

Since $r_m \approx r_o$

$$(36a)\quad \frac{\sigma_m}{\sigma} = \frac{\left\{r_m+d_o-\frac{2}{\sqrt{\pi}}\sqrt{Dt}\right\}^3}{r_m^3}$$

This can be rearranged to give

$$(37)\quad r_m\left\{\left(\frac{\sigma_m}{\sigma}\right)^{\frac{1}{3}}-1\right\} = d_o - \frac{2}{\sqrt{\pi}}\sqrt{Dt} = d(t)$$

If d(t) is plotted vs. $\sqrt{t}$, a straight line is obtained with slope $-2\sqrt{\frac{D}{\pi}}$ and intercept d_o. When $t = t_1$, the line will no longer be straight and at this point

$$(38)\quad d(t_1) = h$$

The tensile strengths obtained after the gold oxide has been reduced to a monolayer could not be directly measured since they exceed the tensile strengths of the gold and the sapphire. The analysis has been carried this far only for the sake of completeness.

The experimental data are given in Table 5 and plotted in Figure 15. Since it is assumed that oxygen is the rate controlling species in the diffusion of gold oxide into sapphire, the diffusion coefficients calculated for each temperature and tabulated in Table 6 are plotted along with the data given by Kingery and Oishi[54] for oxygen self diffusion in sapphire in Figure 16.

TABLE 6

CALCULATED DIFFUSION COEFFICIENT

T (^oK)	D (cm^2/sec)
1373	1.29×10^{-19}
1423	4.24×10^{-19}
1473	7.60×10^{-19}

The data points in the upper left in Figure 17 are some of the points reported by Kingery and Oishi, The line through these points is a plot of their equation

TABLE 5

THICKNESS OF THE CONTAMINATING LAYER OF GOLD OXIDE FOR VARIOUS TIMES AT THREE TEMPERATURES

1100°C

3600	60.0	2860	202.0	5.86	4.86	12.12
15,000	122.2	6000	96.4	4.58	3.58	8.94
27,000	164.0	7380	78.4	4.28	3.28	8.20
32,400	180.0	4890	118.0	4.90	3.90	9.75
33,600	183.8	7990	72.5	4.16	3.16	7.90

1150°C

3600	60.0	4610	125.2	5.01	4.01	10.00
4200	64.7	3660	159.1	5.41	4.41	11.00
4980	70.5	3760	158.6	5.41	4.41	11.00
5400	73.4	3340	173.1	5.56	4.56	11.40
7680	87.5	4200	137.8	5.16	4.16	10.40
16,200	127.0	4740	122.0	4.96	3.96	9.90
24,000	155.0	7620	75.8	4.22	3.22	8.05

1200°C

3600	60	7040	82.3	4.35	3.35	8.37
5100	71.4	9750	59.3	3.90	2.90	7.25
5700	75.5	5360	107.9	4.76	3.76	9.40
6900	83.0	3860	149.9	5.31	4.31	10.77
7800	88.4	5100	113.4	4.84	3.84	9.60
9900	99.5	5660	102.0	4.67	3.67	9.16

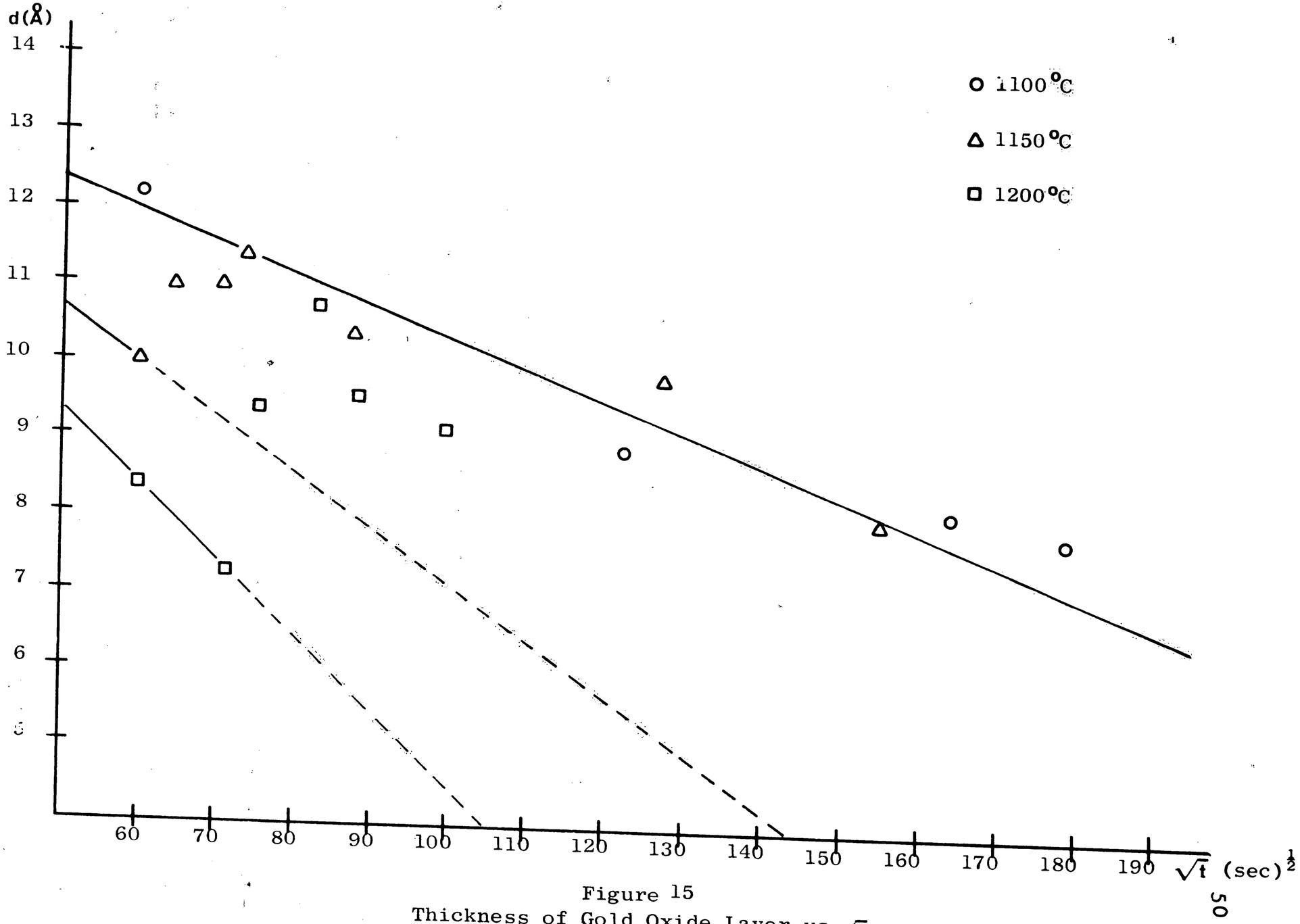

Figure 15
Thickness of Gold Oxide Layer vs $\sqrt{t}$.

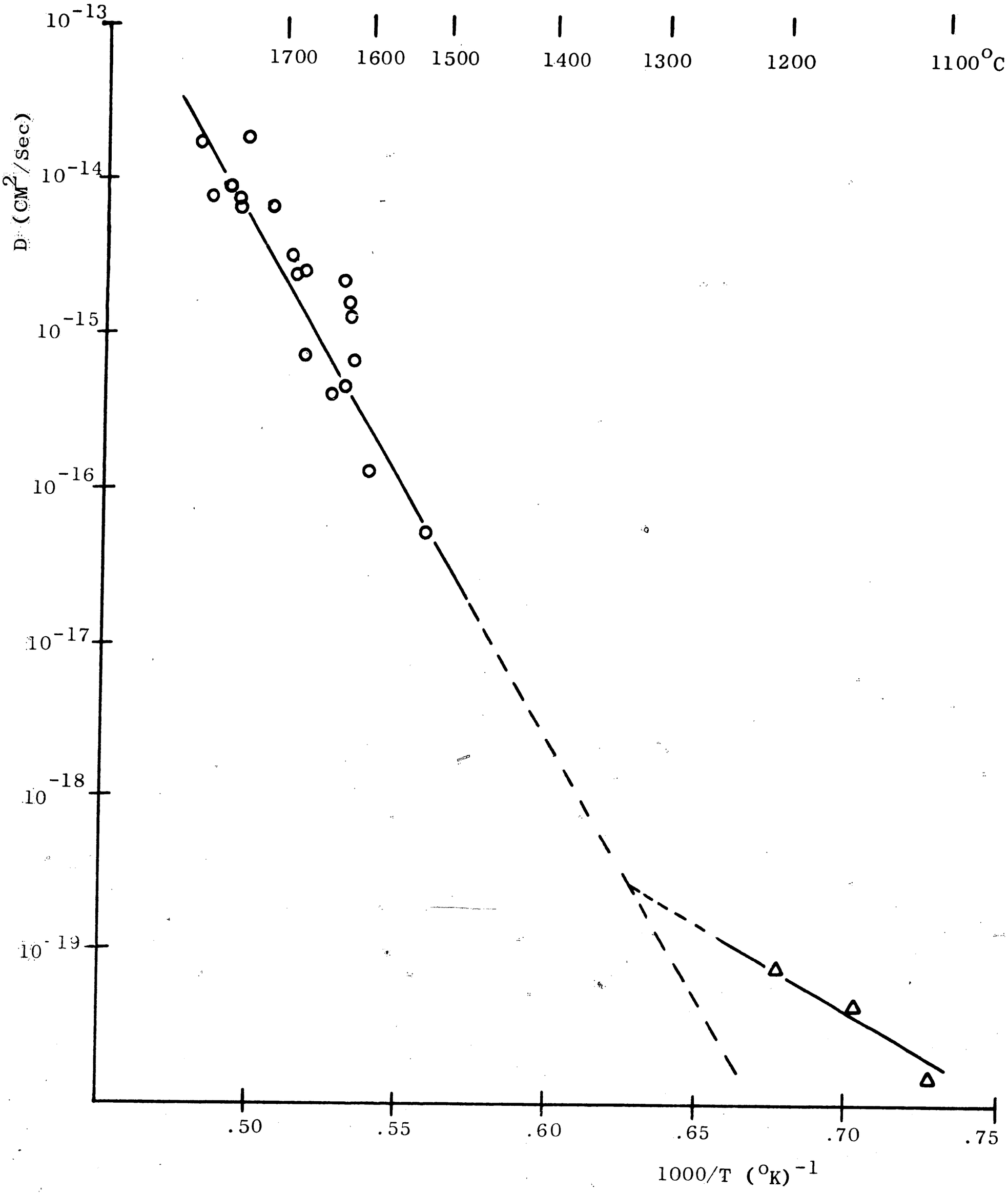

Figure 16
D vs 1000/T

$$(39)\quad D = 1.9 \times 10^{3} e^{-152{,}000/RT}$$

It appears that at the temperatures used in this investigation the diffusion coefficient is in the extrinsic range. Kingery and Oishi also obtained some data for diffusion in the extrinsic range. They measured an activation energy for ion mobility of 57,600 calories per mole. From the slope of the line in Figure 17, the activation energy measured in this investigation is 47,800 calories per mole. The line can be represented by the equation

$$(40)\quad D = 5 \times 10^{-11} e^{-47{,}800/RT}$$

Since the data of Kingery and Oishi were well represented by

$$(41)\quad D = 6.3 \times 10^{-8} e^{-57{,}000/RT}$$

it appears that the sapphire disks used in this experiment had less defects in them than the crushed grain samples used by Kingery and Oishi. There is one other possibility, however. In a sapphire crystal the diffusion coefficient is dependent upon the direction of the gradient. Kingery and Oishi's results are an average from a large number of randomly oriented crystals while the results of this investigation pertain to diffusion in a single direction. It would be interesting to measure the diffusion coefficient for several crystallographic orientations.

The value of 14.4 $\mathring{A}$ obtained for d_o, the initial thickness of the gold oxide layer, and the measured values of D do not seem unreasonable.

Unfortunately, some other mechanism begins to operate in the 1150°C and 1200°C experiments. The details of this mechanism have not been determined but it is possible that the vapor pressure of the gold oxide becomes very high at these temperatures causing the interface to become unstable. It is also possible that oxygen diffuses into the interface more rapidly than gold oxide diffuses away at these temperatures.

The last task of this section will be to predict the tensile strength of a gold/sapphire bond formed in an oxygen atmosphere as a function of time and temperature. From equation (33)

$$\sigma = -\frac{K}{\left\{r_o + d_o - \frac{2}{\sqrt{\pi}}\sqrt{Dt}\right\}^3} = -\frac{K}{\left\{r(T,t)\right\}^3}$$

The data are plotted in Figure 17. The experimental data are superimposed on the plot of σ vs $\sqrt{t}$.

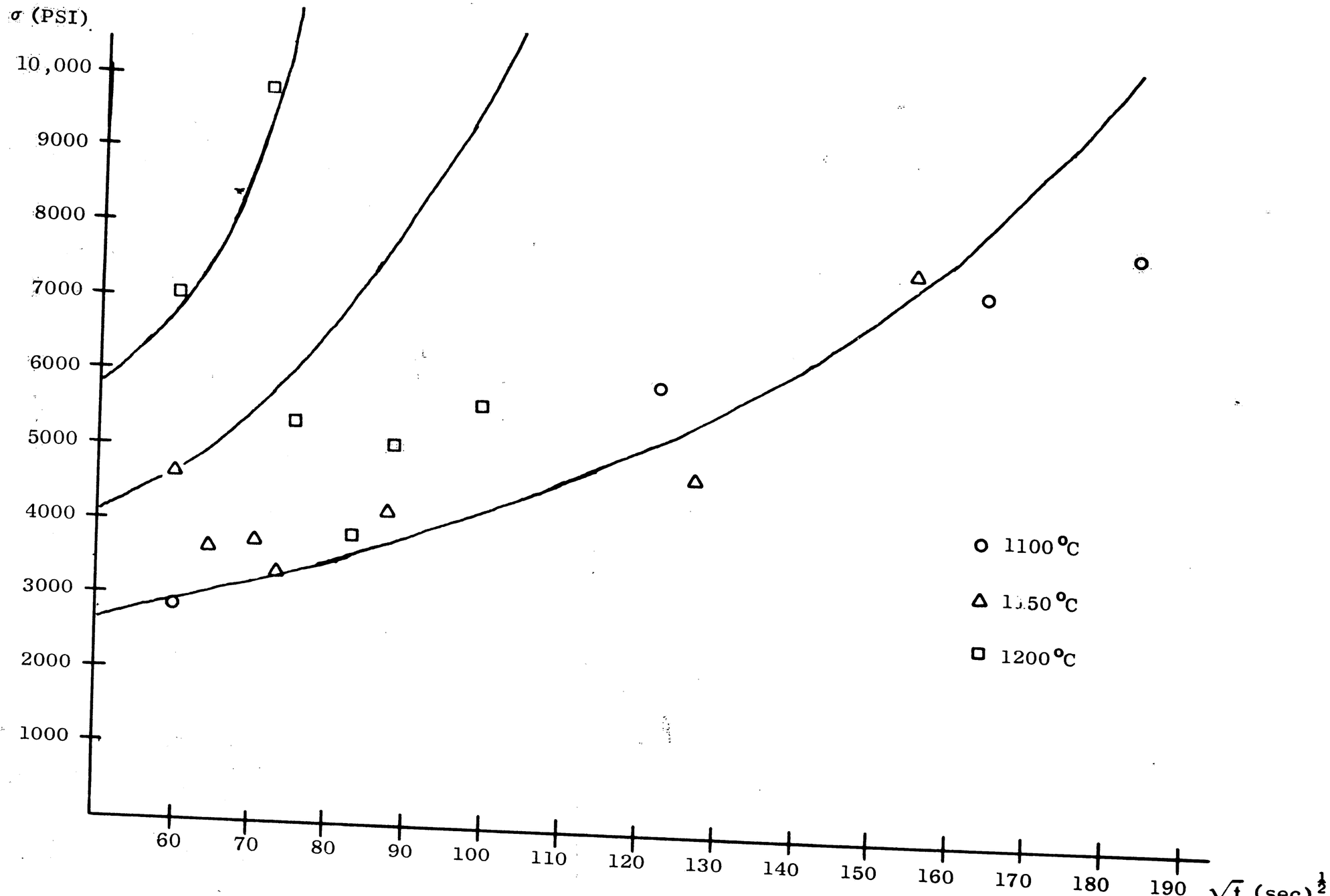

Figure 17

Theoretical σ vs $\sqrt{t}$ Curves for 1100°, 1150°, and 1200° with Actual Data Superimposed.

VI. SUMMARY AND CONCLUSIONS

As a result of this investigation a technique has been developed for tensile testing sessile drops and an equation has been developed for the tensile strength of a bond between a metal an ionic solid when the bond is composed only of dispersion forces. This equation shows that the tensile strength of such a metal/ceramic bond is dependent only on the chemical compositions and densities of and the separation between the metal and the ceramic. In the special case where the bond has been formed between gold and smooth aluminum oxide in an oxygen atmosphere, the separation between the gold and aluminum oxide has been theoretically determined as a function of time and temperature. Application of the derived equations to the experimental results has led to a calculation of the diffusion coefficient for oxygen self diffusion in sapphire. The observed temperatures dependence of the diffusion coefficient has led to a determination of the activation energy for ion mobility that agrees well with the value given by Kingery and Oishi. The model explains the effect of oxygen on the tensile strength of the bond and the extremely high tensile strength of the bond near the perimeter of the two phase interface.

The model appears to break down at higher temperatures and additional work needs to be done to determine the reason. Also, the precision of the measurements is probably not high due at least partly to an inadequate testing fixture. Any further work should be done with more sophisticated equipment. It would also be of interest to extend the model to other noble metal/ceramic systems.

APPENDIX I

THE THEORY OF ADHESION BY VAN DER WAALS FORCES

Van der Waals forces are secondary forces that exist between atoms or molecules in addition to any forces due to ionic, covalent, or metallic bonds. It has become apparent that the so called van der Waals forces are really several different kinds of forces, one or more of which are acting in any given system.

In a system of molecules with permanent dipole moments, the molecules will tend to line up positive end to negative end. This is what is known as the orientation effect. In 1912 Keesom[1] showed that the average potential energy between two molecules due to the orientation effect was given by

(1) $\overline{U} = -\frac{2}{3}\frac{\mu_I^2 \mu_{II}^2}{R^6}\frac{1}{kT}$ when $\frac{\mu_I \mu_{II}}{R^3} \ll \frac{1}{kT}$

(2) $\overline{U} = -\frac{2\ \mu_I \mu_{II}}{R^3}$ $\frac{\mu_I \mu_{II}}{R^3} \gg \frac{1}{kT}$

μ_I is the dipole moment of molecule I

R is the distance between the two molecules

k is Boltzmann's constant

T is the Kelvin temperature

(In this discussion U ($R = \infty$) = 0 and all units are cgs.)

In 1920, Debye[2] investigated the effect of a polar molecule on the electron cloud of another molecule, the induction effect. He succeeded in proving that the average potential energy between two molecules due to the induction effect was given by

(3) $\bar{U} = -\frac{1}{R^6}\left[a_{\perp}\mu_{\perp}^2 + a_{\parallel}\mu_{\perp}^2\right]$ where

R is the distance between the molecules

a is the polarizability of the particular molecule

μ is the dipole moment of the particular molecule

In 1930, London[3,4] realizing the inadequacy of the orientation effect and the induction effect to account for all the van der Waals type forces observed, turned to quantum mechanics and showed that there are interactions between atoms and molecules not predicted by classical physics. These interactions he termed the dispersion effect. This effect does not depend on the existence of permanent dipoles or quadrupoles or any higher order poles. London succeeded in showing that the potential energy between any two molecules or atoms or ions due to the dispersion effect is given by

(4) $U = -\frac{3}{2}\frac{a_{\perp}a_{\parallel}}{R^6}\frac{J_{\perp}J_{\parallel}}{J_{\perp}+J_{\parallel}} = -\frac{C}{R^6}$ provided that

(4a) $a_{\perp} < R^3$ and $a_{\parallel} < R^3$ where

a is the polarizability of the particular atom or molecule or ion

J is the characteristic energy of the particular atom, molecule, or ion

R is the distance between the atoms, molecules, or ions

C is called the dispersion constant

(4b) $J = h\nu_0$ where

ν_0 is the characteristic frequency of the atom or molecule or ion

When J is unknown, the relation

(4c) $J \approx I$ where I is the ionization of the atom, molecule or ion

can be used.

The most significant thing about the potential function arising from the dispersion effect is that it is additive, i.e., if an atom is in the neighborhood of two others, the potential that it sees is the sum of the potentials due to each of its neighbors individually.

In the case of a neutral atom or non polar molecule in the neighborhood of an ionic crystal, there is an additional attraction due to the stationary dipoles of the crystal inducing a dipole in the neutral atom or non polar molecule. This is known as the influence effect. It has been shown by Lenel[4] and Orr[5] that the influence effect is negligible in comparison to the dispersion effect.

At short distances there are repulsion effects between atoms or molecules or ions due to both coulombic repulsion and a force that arises from the exclusion principle. It has been shown[6] that the potential due to these repulsion effects is given by

(5) $U = b\, e^{-R/\rho}$ where

b and ρ are constants for each system

R is the distance between the atoms, molecules, or ions

It is of interest to this paper to calculate the potential energy of a system consisting of a neutral atom approaching the surface of an ionic crystal. Since the orientation effect and the

induction effect do not apply in this case and the influence effect can be considered negligible, it remains only to calculate the attraction potential due to the dispersion effect. Since the contributions from individual atoms are additive in this case, one only has to sum the contributions from each ion in an infinite crystal. If $r > (N_c)^{-\frac{1}{3}}$ where r is the perpendicular distance of the adsorbed atom from the crystal and N_c is the ion density of the crystal, the summation over the ions of the crystal can be replaced by an integration over the volume of the crystal. Hence, the attraction potential is given by

$$(6)\quad \varphi_A = \int_{vol} -\frac{N_c C}{R^6}\, dv = -N_c C \left\{ \int_r \int_{-\infty}^{\infty} \int_{-\infty}^{\infty} \frac{dx\, dy\, dz}{\left[x^2+y^2+z^2\right]^3} \right\}$$

The triple integral can be evaluated by the substitutions

$$x^2 = \left[y^2+z^2\right] \tan^2\theta \qquad y^2 = z^2 \tan^2\theta$$

The result is

$$(7)\quad \varphi_A = -\frac{N_c \pi}{6}\,\frac{C}{r^3} = -\frac{C'}{r^3}$$ where

C' is called the adsorption constant

If the crystal is composed of ions of two species, 1 and 2, then the dispersion forces contribute two terms to the attraction potential.

$$(7a)\quad \varphi_A = \varphi_{A_1} + \varphi_{A_2} = -\frac{C_1'}{r_1^3} - \frac{C_2'}{r_2^3}$$

However, one term is usually very much smaller than the other. The negative ions have polarizabilities an order of magnitude larger than the positive ions and, since the negative ions are usually on the surface, the distance to the first negative ion layer is shorter. Hence, the second term is usually neglected and φ_A is approximated by φ_{A_1} . Since the repulsive forces are very short range forces, the sum of the potentials of the repulsion type has significant contributions only from the nearest neighbors to the adsorbed atom. Since the nearest neighbors are all at the same distance

(8) $\varphi_R = n' b e^{-R/\rho}$ Where

n' is the number of nearest neighbors

To find the adsorption energy due to repulsive forces in terms of the distance from the crystal surface rather than the distance to the nearest neighbors, R must be expressed in terms of r.

To a first approximation,

(9) $R \approx r$ when $r > (N_c)^{-\frac{1}{3}}$

Let

(10) $n' b = B$

Then

(11) $\varphi_R = B e^{-r/\rho}$

The adsorption energy of an atom near the surface of an infinite crystal is given by

(12) $\Phi = B e^{-r/\rho} - \frac{C'}{r^3}$

Since the adsorption energies are additive, the adsorption energy per unit area for a monolayer of atoms near the surface of a crystal is given by

$$E = n\,\Phi \qquad (13)$$

where

n is the number of adsorbed atoms per unit area

If a second layer of atoms is spread on top of the first, it will be attracted to the crystal also, but the adsorption energy will be less. Let the adsorption energy of the first layer be E_1 and of the jth layer be E_j. Then

$$E_1 = E(r_1) \qquad (14)$$

and

$$E_j = E(r_j) \qquad (14a)$$

The total adsorption energy for many atomic layers on the crystal is given by the sum of the energies for each layer. Thus

$$E = \sum_{j=1}^{\infty} E_j \qquad (15)$$

It will be convenient to break up the adsorption energy of a metal near the surface of a crystal into the part due to the attractive forces and the part due to the repulsive forces. Thus

$$E = \sum_{j=1}^{\infty} (E_A + E_R)_j = \sum_{j=1}^{\infty} E_{A_j} + \sum_{j=1}^{\infty} E_{R_j} = E_A + E_R \qquad (16)$$

$$E_{R_1} = n\,B\,e^{-r/\rho} \qquad (17)$$

where

r is the distance of the first atomic layer from the crystal surface

Since the repulsive forces are extremely short range forces we can assume that $E_{R2} = E_{R3} = \ldots = E_{Rj} = \ldots = 0$ and

(18) $E_R = E_{R1}$

If $r > d'$ where d' is the distance between the atomic layers of adsorbed atoms, the summation over the layers can be replaced by an integration over the volume of the adhering metal. Thus

$$(19)\quad E_A = \frac{1}{d'}\int_r^\infty E_A(x)\,dx = \frac{n}{d'}\int_r^\infty \varphi_A(x)\,dx$$

Substituting equation (7) into (19)

$$(20)\quad E_A = -\frac{n}{d'}\int_r^\infty \frac{C'}{x^3}\,dx$$

$$(21)\quad E_A = -\frac{1}{2}\,\frac{n}{d'}\,\frac{C'}{r^2} \qquad \text{But} \qquad (22)\quad \frac{n}{d'} = N_M \qquad \text{where}$$

N_m is the number of metal atoms per unit volume.

Substituting equations (17), (18), (21), and (22) into (16)

$$(23)\quad E = nBe^{-r/\rho} - \frac{1}{2}N_M\frac{C'}{r^2}$$

E, E_A, and E_R are plotted vs. r in Figure 1.

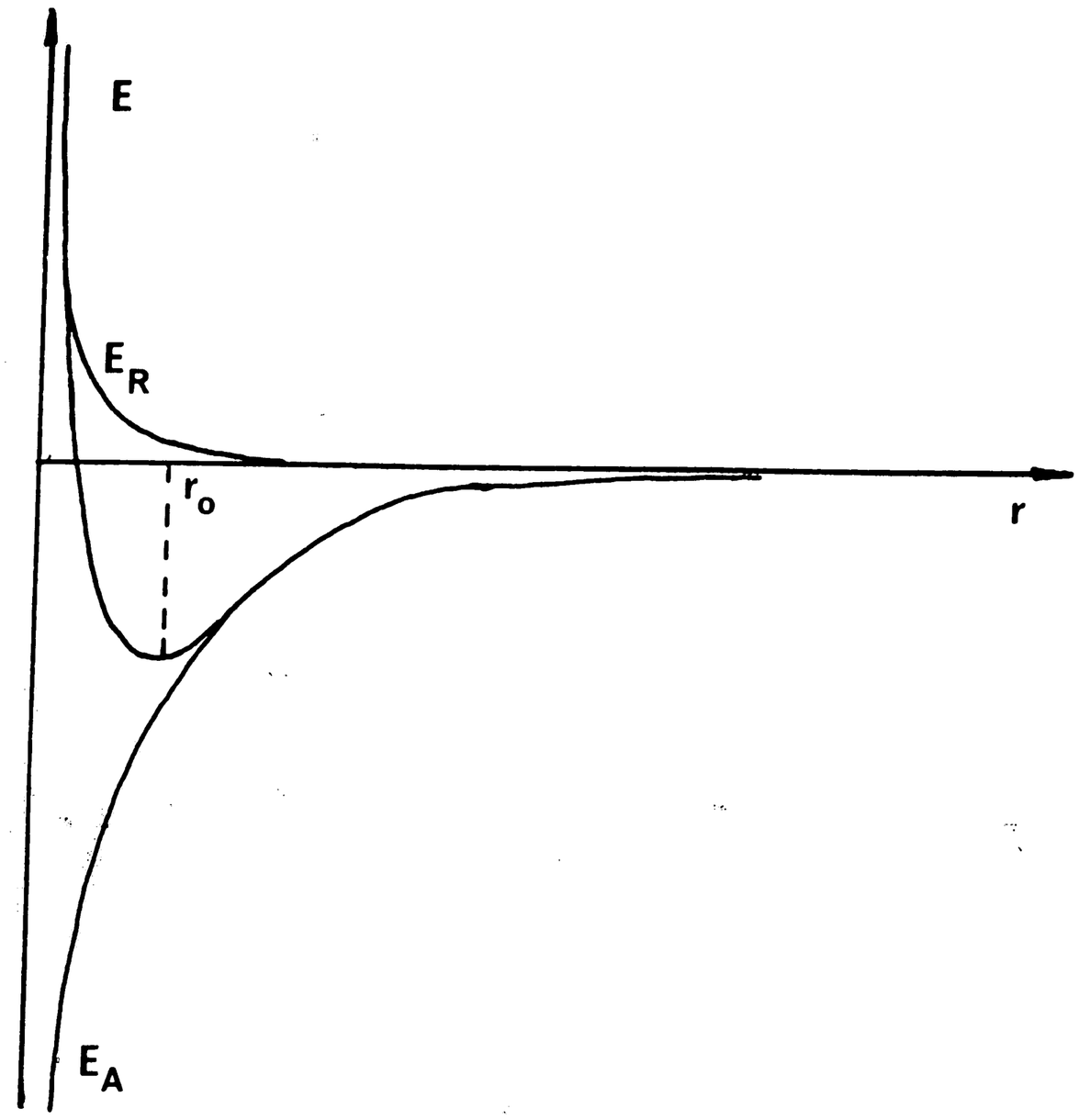

FIGURE 1

If the surface of the metal and the crystal were clean on an atomic scale, the metal would come to rest at the point where $\frac{dE}{dr} = 0$. This point will be defined to as r_o. If all the constants in equation (23) were known for the gold/sapphire system, r_o could be found directly by setting $\frac{dE}{dr} = 0$ and solving for $r = r_o$. Unfortunately, B and ρ are not known for the system so r_o cannot be calculated from equation (23). This is not crutial, however, since the quantity of interest to this thesis is not the adsorption energy but rather the maximum tensile stress the adhesive bond will support. The force acting on any body in a potential field is the negative of the potential gradient. A force of this magnitude and in the opposite direction must be applied to move the body against the gradient.

The magnitude of the potential gradient is in general a function of position and it has a maximum at some point.

$$(24)\quad \vec{F} = -\nabla\Omega$$

If the potential energy Ω is given as an energy per unit area, then the force is also per unit area, i.e. a stress. Thus

$$(25)\quad \vec{\sigma} = -\nabla E$$

Since the gradient is in the r direction for this system, equation (25) can be replaced by

$$(26)\quad \sigma = -\frac{\partial E}{\partial r}$$

Since the breaking stress of the bond is required, the stress of interest is

$$(27)\quad \sigma_{max} = -\left.\frac{\partial E}{\partial r}\right]_{max}$$

Thruout this paper, whenever σ is used, σ_{max} is implied.

Equation (26) cannot be used directly since all the constants in equation (23) would have to be known. However, due to the fact that the repulsive forces are of such a short range, the walls of the potential well (E vs r) are very steep, and the maximum slope of E (r) is reached at a point only slightly greater than r_o. This slope is very nearly equal to the slope of the E_A vs r curve at the same point. Since all the constants are known in equation (21), the only information necessary to calculate σ (σ_{max}) for the gold/sapphire system is an estimate of r_m, the point of maximum $\frac{\partial E}{\partial r}$. The situation is shown in the graph below:

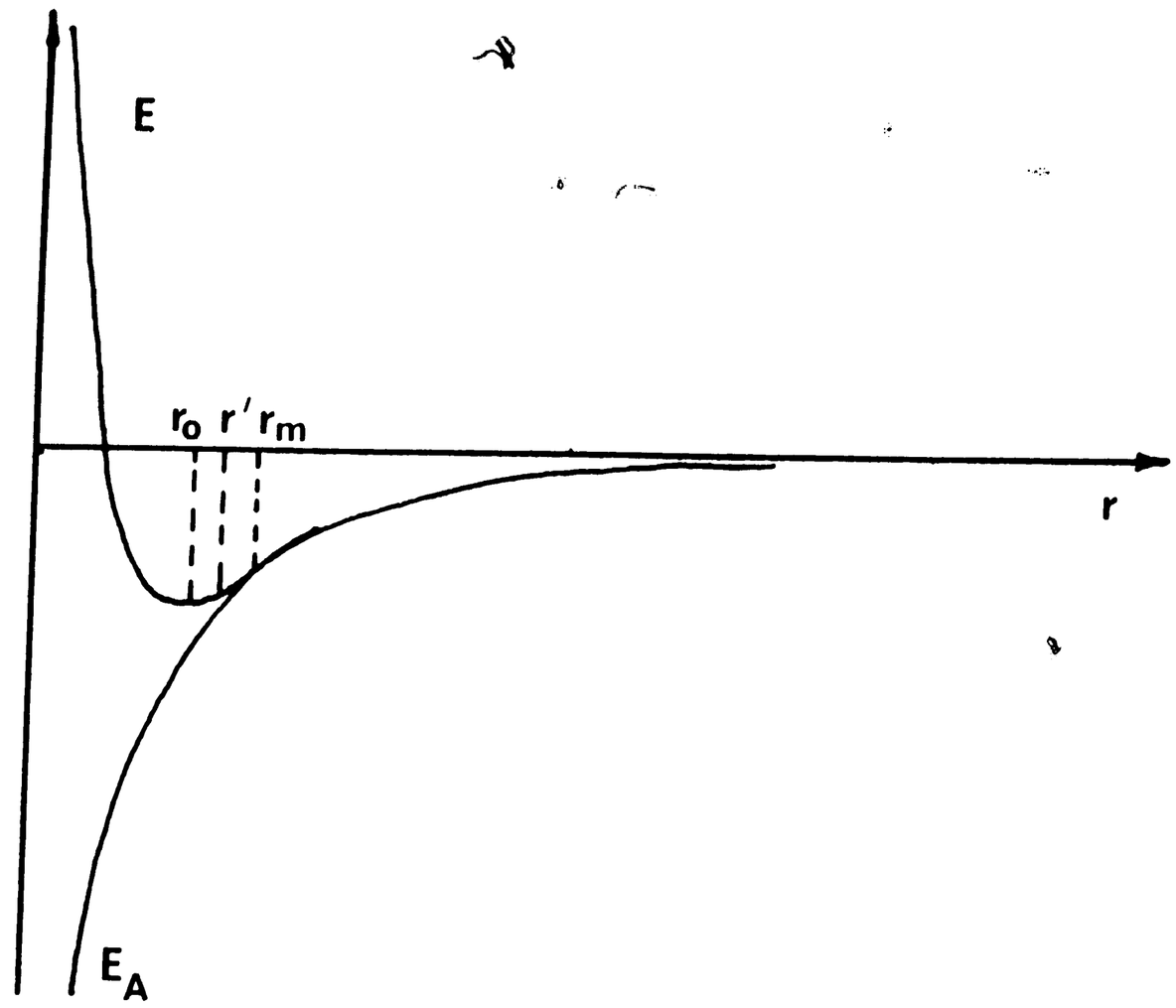

FIGURE 2

One way of estimating r_m would be to estimate r_o and assume a slightly larger value for r_m. Benjamin and Weaver[7] assume that r_o is the sum of the radii of the metal atoms and the crystal ions. This seems a reasonable first approximation but there is a better way to estimate r_m that does not involve estimating r_o first. The quantity $E(r_0)$ is the adsorption energy of a metal on the surface of a clean crystal. This quantity is usually referred to in papers on adhesion as the work of adhesion and is designated W_{AD}. (For a discussion of adhesion from a thermodynamic point of view, see Appendix II). The work of adhesion for gold on aluminum oxide has been measured very precisely by Pilliar and Nutting[8]. If W_{AD} were substituted for E_A in equation (21), r' could be obtained as

$$(28) \quad r' = \sqrt{\frac{N_M C'}{2 W_{AD}}}$$

(The work of adhesion is usually given as a positive quantity but the sign convention in this appendix required $W_{AD} = E(r_o)$ to be negative. This takes care of the minus sign in equation (21).)

As seen in Figure 2, r' lies between r_o and r_m. Thus, r' is a better estimate of r_m than r_o. In order to calculate r' it is necessary to know the values of the constants in equation (28). These values are tabulated below.

Constant	Value	Units	Source
N_O=	2.13×10^{23}	Cm^{-3}	-
a_{Au}	1.286×10^{-24}	Cm^3	-
a_O=	3.88×10^{-24}	Cm^3	7
J_{Au}	1.48×10^{-11}	ergs	9
J_O=	8.8×10^{-11}	ergs	7
C'	1.056×10^{-35}	ergs Cm^3	-
N_{Au}	5.9×10^{-22}	Cm^{-3}	-
m	9.108×10^{-28}	gm	-
h	6.625×10^{-27}	erg sec	-
e	4.803×10^{-10}	escoulomb	-
W_{AD}	530	erg Cm^{-2}	8

For a neutral atom the polarizability is calculated from the formula[5]

$$(29)\quad \alpha = \frac{e^2 h^2}{4\pi^2 m I^2}$$ where

I is the ionization potential of the atom

The oxygen ion density is calculated from a knowledge of the structure of sapphire. Sapphire can be considered to be a hexagonal close packed array of oxygen ions with 2/3 of the octahedral sites filled with aluminum ions. This unit cell of oxygen ions (not the unit cell of the sapphire crystal) has parameters $a_o = 2.74$ Å and $C_o = 4.33$ Å. Thus

$$(30)\quad N_c = \frac{12}{\sqrt{3}\, a_o^2 c_o} = 2.13 \times 10^{23} \text{ ions per cm}^3$$

The gold atom density is calculated from a knowledge of the structure of gold, which is fcc with a lattice parameter of 4.0783Å. Hence

$$(31)\quad N_M = \frac{4}{a_o^3} = 5.90 \times 10^{22} \text{ atoms per cm}^3$$

From equation (28)

$$(32)\quad r' = 2.42 \times 10^{-8} \text{ cm}$$

Since r_m is slightly greater than r', let

$$(32a)\quad r_m = 2.5 \text{ Å}$$

To check the reasonableness of the value used for r_m, consider that Benjamin and Weaver would estimate $r_o = r_{Au} + r_{O^=} = 1.44 \text{ Å} + 1.37 \text{ Å} = 2.81 \text{ Å}$ If the gold atoms were considered to be hard spheres resting above the centeroids of the equalateral triangles formed by a close packed plane of oxygen ions, then r_o would be given by

(33) $r_o = \sqrt{(r_{O^=} + r_{Au})^2 - a^2}$ where

$$a = \frac{2}{3}\sqrt{3}\ r_{O^=}$$

This gives $r_o = 2.32\text{Å}$. The calculated value of r' is about halfway between these two values.

It is now possible to calculate the tensile stress which the adhesive bond between clean atomically flat gold and sapphire will support. From equation (21)

(34) $\sigma = -\frac{\partial E_A}{\partial r} = -\frac{N_M C'}{r^3} = -\frac{K}{r^3}$ where

K is called the adhesion constant

Hence

(35) $\sigma_m = -\frac{K}{r_m^3} = -3.98 \times 10^{10}$ dynes per cm^2 or

(35a) $\sigma_m = -5.78 \times 10^5$ pounds per in^2 since

(36) 1 dyne per $cm^2 = 1.45 \times 10^{-5}$ pounds per in^2

Before concluding the discussion of van der Waals bonding between a metal and a crystal, it would be wise to go back and check the assumptions made for the validity of the equations used. Equation (4) was valid only with the stipulation that a_I and a_{II} were both less than R^3. The smallest R ever gets is r_m.

$$r_m^3 = 1.22 \times 10^{-23}\ cm^3$$

This is greater than either a_{Au} or $a_{O^=}$.

In equation (7a) it was pointed out that the attraction potential was composed of two terms but that one was very much smaller than the other. To show that this is indeed the case for aluminum oxide it is necessary to know the aluminum ion density of sapphire, the polarizability of the aluminum ion, and the distance between the gold and first layer of aluminum ions. From Van Vleck[10]

$$\kappa = .15 \ \frac{cm^3 \, atom}{gm \ atom}$$

and

$$\alpha = \frac{3\kappa}{4\pi L}$$

where

L is Avogadro's number

Hence

$$\alpha_{Al^{+++}} = 5.95 \times 10^{-26} \ cm^3$$

$$N_{Al^{+++}} = \frac{2}{3} N_{O^{=}} = \frac{2}{3} N_C$$

Therefore

$$C_2' = .0102 \ C_1'$$

From Dils[11]

$$r_2 = r_1 + 1.077 \ \text{Å}$$

Therefore

$$\varphi_{A_2} = \frac{.0102 C_1'}{(r_1 + 1.077 \times 10^{-8})^3} < .01 \ \varphi_{A_1}$$

The integration in equation (6) was only valid where $r > (N_c)^{-\frac{1}{3}}$.

Since the smallest r ever gets is r_m, r_m must be greater than $(N_c)^{-\frac{1}{3}}$.

$$(N_c)^{-\frac{1}{3}} = 1.68 \times 10^{-8} \text{ cm} < r_m$$

Finally, the integration of equation (19) was only valid if $r > d'$.

Since the smallest r ever gets is r_m, r_m must be greater than d'.

In a cubic crystal, the interplanar spacing is given by

$$(37) \quad d'_{hkl} = \frac{a_o}{\sqrt{h^2+k^2+l^2}}$$

The atomic planes which are the farthest apart are the (110) planes. Unfortunately,

$$d'_{110} = 2.88 \text{ Å} > r_m$$

However, this is very near to r_m and all other planes have spacings which are smaller than r_m. If any contaminating layer is between the gold and sapphire, r will always be greater than d'_{max}.

To summarize, an equation has been derived for the tensile stress that an adhesive bond between a metal and an ionic crystal will support when the only bonds are van der Waals bonds of the dispersion type. This equation shows that the tensile stress the bond will support (maximum bond stress) is independent of the orientation of the crystallographic planes of the system components, in fact the components may even be polycrystalline or amorphous. It is important to note that the critical assumption is that both surfaces are clean on an atomic scale and that there are no stresses permanently supported at the interface. The maximum bond stress has been evaluated for the gold/sapphire system. The result indicates that maximum bond stress

of a perfect bond could never be directly tested since its magnitude is greater than the tensile strength of both gold and sapphire.

$$\sigma_m = 578,000 \quad \text{PSI}$$

(37)

$$\sigma_{Au} = 30,000 \quad \text{PSI}$$

$$\sigma_{Al_2O_3} = 65,000 \quad \text{PSI}$$

1. W. H. Keesom, LEIDEN. COMM. SUPPL. 1912, 24a, 24b, 25, 26; 1915, 39a, 39b, PROC. AMST., 1913, Vol. 15, 240, 256, 417, 643; 1916, Vol. 18, 636; 1922, Vol. 24, 162. PHYSIK. Z. , 1921, Vol. 22, 129, 643; 1922, Vol. 23, 225.

2. P. Debye, PHYSIK. Z ., 1920, Vol. 21, 178; 1921, Vol.22, 302

3. F. LONDON, Z. PHYSIK. CHEM., 1930, B, 11, 222

4. F. LONDON, TRANS. FARADAY SOC., 1937, 33, 8

5. F. V. LENEL, Z. PHYSIK. CHEM., 1933, B, 23, 379

6. W. J. C. ORR, TRANS. FARADAY SOC., 1939, 35, 1247

7. P. BENJAMIN AND C. WEAVER, PROC. ROY, SOC. (LONDON), 1959, A, 252, 418

8. R. M. PILLIAR AND J. NUTTING, PHIL. MAG., 1967, 16, 181

9. W. FINKELBURG AND W. HUMBACH, NATURWISSENSCHAFTEN, 1955, 42,35

10. J. H. VAN VLECK,"THE THEORY OF ELECTRIC AND MAGNETIC SUSCEPTIBILITIES" OXFORD UNIVERSITY PRESS, AMEN HOUSE, E.C. 4, 1932, P 216 and P 222.

11. R.R. DILS, "CATION INTERDIFFUSION IN THE CHROMIA-ALUMINA SYSTEM" Ph.D. THESIS, STANFORD UNIVERSITY, 1965, P 47

APPENDIX II

ADHESION FROM A THERMODYNAMIC POINT OF VIEW

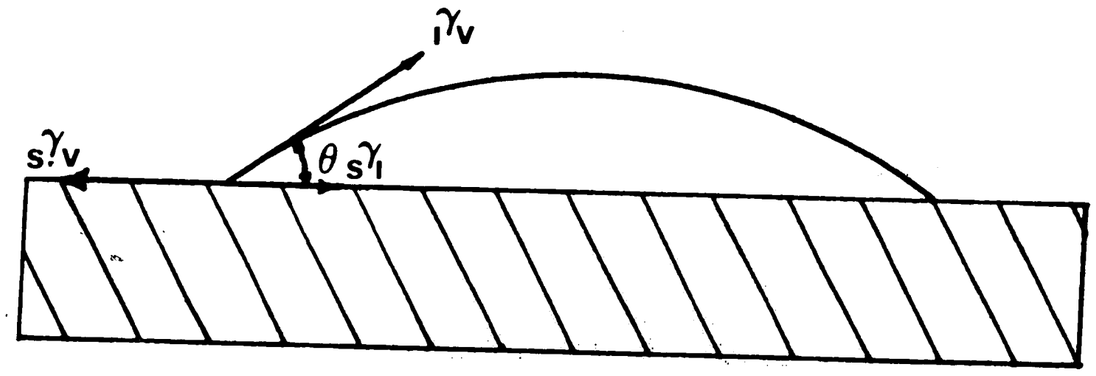

SESSILE DROP

When a drop of liquid is resting on a solid substrate and equilibrium has been reached between the phases of the system, i.e., between the liquid, solid, and vapor, the liquid drop will have a contact angle with the substrate such that the forces are balanced at the three phase interface. This angle is given by Young's equation:

$$(1) \qquad {}_s\gamma_v = {}_s\gamma_l + {}_l\gamma_v \cos\theta$$

where s, l, and v refer to the solid, liquid, and vapor phases respectively, γ is the interfacial tension between the phases denoted by the subscripts, and θ is the contact angle measured inside the drop. Equation (1) can be rearranged to obtain

$$(2) \qquad {}_s\gamma_v - {}_s\gamma_l = {}_l\gamma_v \cos\theta$$

The free energy of formation of the liquid-solid interface is

given by

$$(3)\quad \Delta F = {}_sF_l - [{}_lF_v + {}_sF_v]$$

where

F is the Gibbs free energy per unit area of the interface denoted by the subscripts.

It will now be shown that for the case of a liquid and solid that do not mix $F = \gamma$

Let the Gibbs free energy of the system be composed of two parts, one part due to reversible contributions to the free energy (the reversible contact of the liquid to the solid) and the other part due to contributions that are inherently irreversible in nature, i.e., mixing of the two phases.

Then

$$(5)\quad G = G_1 + G_2$$

where

$$(6)\quad G_1 = E + PV - TS$$

(reversible part)

$$(7)\quad G_2 = \left\{\bar{G}_1N_1 + \bar{G}_2N_2\right\}_{\text{solid phase}} + \left\{\bar{G}_1N_1 + \bar{G}_2N_2\right\}_{\text{liquid phase}}$$

(mixing part)

$$(8)\quad dG = dE + PdV + VdP - TdS - SdT + \left\{\bar{G}_1dN_1 + \bar{G}_2dN_2\right\}_{lp} + \left\{\bar{G}_1dN_1 + \bar{G}_2dN_2\right\}_{sp} + \left\{N_1d\bar{G}_1 + N_2d\bar{G}_2\right\}_{lp} + \left\{N_1d\bar{G}_1 + N_2d\bar{G}_2\right\}_{sp}$$

$$(9)\quad N_1d\bar{G}_1 + N_2d\bar{G}_2 = 0$$

(Gibbs-Duhem relation)

If the only work done in expanding an interface is done against the interfacial tension, then

$$(10)\quad \delta W = -\gamma\, dA$$

where

W is the work done by the system

A is the area of the interface

From the first law

(11) $\delta W = \delta q - dE$

From the second law

(12) $\delta q_R = TdS$ where

q_R is the heat absorbed in a reversible way

From (10), (11), (12)

(13) $dE = \delta q - \delta W = TdS + \gamma dA$

Substituting (13) and (9) into (8)

(14) $dG = \gamma dA + PdV + VdP - SdT + \{\bar{G}_1 dN_1 + \bar{G}_2 dN_2\}_{lp} + \{\bar{G}_1 dN_1 + \bar{G}_2 dN_2\}_{sp}$

At constant T, P, and V

(15) $dG = \gamma dA + \{\bar{G}_1 dN_1 + \bar{G}_2 dN_2\}_{lp} + \{\bar{G}_1 dN_1 + \bar{G}_2 dN_2\}_{sp}$

If the two components do not mix

(16) $dN_1 = dN_2 = 0$ in both phases and

(17) $dG = \gamma dA$

If γ is constant over the area of the interface

(18) $\int_0^G dG = \gamma \int_0^A dA$ and

$G = \gamma A$ or

(19) $\gamma = \frac{G}{A} = F$

Hence:

(20)
$$_lF_v = {}_l\gamma_v$$
$$_sF_v = {}_s\gamma_v$$
$$_sF_l = {}_s\gamma_l$$

If we define the work of adhesion as the work necessary to remove the interface between the solid and liquid, and replace it by solid-vapor and liquid vapor interfaces, we can show that

(21) $W_{AD} = -\Delta F$ where

W_{AD} is the work of adhesion

(22) $F = E + PV - TS$ where the quantities

are in appropriate units per unit area and no mixing takes place. At constant temperature, pressure, and volume

(23) $\Delta F = \Delta E - T\Delta S$

(24) $\Delta S = \int_0^Q \frac{dq_R}{T} = \frac{Q}{T}$ (from the second law)

Substituting (24) into (23)

(25) $\Delta F = \Delta E - Q$

From the first law

(26) $\Delta E = Q - W$

Substituting (26) into (25)

(27) $\Delta F = Q - W - Q = -W$ where

$W = W_{AD}$

Equation (3) may now be written

(28) $\Delta F = {}_s\gamma_l - \{ {}_l\gamma_v + {}_s\gamma_v \}$

(29) $W_{AD} = -\Delta F = {}_l\gamma_v + {}_s\gamma_v - {}_s\gamma_l$

This is the Dupre equation.

Substituting Equation (2) into Equation (29) we obtain

(30) $W_{AD} = {}_l\gamma_v + {}_l\gamma_v \cos\theta = {}_l\gamma_v \{ 1 + \cos\theta \}$

This is the famous Young-Dupre equation. It is valid so long as the conditions assumed in its derivation are met. The critical conditions are:

(1) equilibrium has been reached, at least on the perimeter of

the interface

(2) there is no mixing of the two phases

The Young-Dupre equation also applies to a solid drop on a solid substrate subject only to the additional condition that no elastic stresses are supported at the interface, thus violating the assumption made in writing equation (10). It is much more difficult to obtain equilibrium conditions with a solid drop, however.

Sometimes the term work of adhesion is used to mean the energy necessary to separate the liquid from the solid in such a way as to leave the surface of the solid not in equilibrium with the vapor of the liquid but with a vacuum (except for whatever vapors of the solid may be present at the temperature in question and the ambient atmosphere.)

Let the surface tension of a solid exposed to a vacuum be denoted by $_s\gamma$. Then

(31) $_s\gamma = {}_s\gamma_v + \phi$

Equation (29) must now be written

(32) $W'_{AD} = {}_l\gamma_v + {}_s\gamma - {}_s\gamma_l$

Substituting (31) into (32)

(33) $W'_{AD} = {}_l\gamma_v + {}_s\gamma_v + \phi - {}_s\gamma_l$

Substituting (2) into (33)

(34) $W'_{AD} = {}_l\gamma_v + \phi + {}_l\gamma_v \cos\theta = {}_l\gamma_v\{1 + \cos\theta\} + \phi$

Substituting (30) into (34)

(35) $W'_{AD} = W_{AD} + \phi$

For the case of liquid gold on solid sapphire $\phi << W_{AD}$

so

(36) $W'_{AD} \approx W_{AD}$

It is of interest to this thesis to show that for the Au/Al_2O_3 system the Young-Dupre equation holds under the conditions of the experiments even though some mixing of the two phases does occur. From equation (5)

$$G = G_1 + G_2$$

and

$$dG = dG_1 + dG_2$$

Since the solutions will be very dilute they are assumed to be ideal. Thus

$$(37)\ \Delta G_{mix} = G_2 - G_2^o = RT\{N_1 \ln N_1 + N_2 \ln N_2\}$$ for each phase

$$(38)\ d\Delta G_{mix} = dG_2 = d\{RT[N_1 \ln N_1 + N_2 \ln N_2]\}$$ for each phase

Hence

$$(39)\ dG = \gamma\, dA + d\{RT[N_1 \ln N_1 + N_2 \ln N_2]\}_{lp} + d\{RT[N_1 \ln N_1 + N_2 \ln N_2]\}_{sp}$$ and

$$(40)\ G = \gamma A + RT\{[N_1 \ln N_1 + N_2 \ln N_2]_{lp} + [N_1 \ln N_1 + N_2 \ln N_2]_{sp}\}$$

Let

N_1 be the mole fraction of gold

N_2 be the mole fraction of aluminum oxide

For an estimate of the mole fraction of each component in each phase, assume that a 15 $\mathring{A}$ layer of gold oxide dissolves in the sapphire and a 1000 $\mathring{A}$ layer of sapphire is dissolved by the gold. Then

$$N_{1lp} \approx 1$$

$$N_{2lp} = 9.2 \times 10^{-5} \qquad (41)$$

$$N_{1sp} = 3.0 \times 10^{-8}$$

$$N_{2sp} \approx 1$$

Substituting these values into equation (40) gives

$$G = 22.7 - 2.26 - .00137 = 20.4 \text{ ergs} \qquad (42)$$

Thus $G \approx \gamma A$

and

$\gamma \approx F$.

Therefore, the Young-Dupre equation is reasonably valid under the conditions of the experiments.

APPENDIX III

DATA

DATA POINTS FROM THE SAMPLES MARKED WITH (*) ARE THE ONES USED IN THE RESULTS SECTION

SAMPLES MARKED WITH (**) FAILED PARTIALLY IN THE SAPPHIRE

RUN #1 Au in O_2 at 1100°C For 1 Hour 40 Min.

No	θ	Pull (Lbs)	Area (In^2)	Stress $\left(\frac{Lb}{In^2}\right)$
1	120°	14.85	.00785	1890
2	125°	9.55	.00864	1110
3	120°	18.95	.00636	2980
4	120°	27.22	.0104	2630
5	120°	23.78	.0113	2110
6	120°	13.64	.00950	1440
7	115°	28.29	.01204	2350
8	125°	10.89	.00565	1930

RUN #2 Au in O_2 at 1100°C For 1 Hour

No	Pull (Lbs)	Area (In^2)	Stress $\left(\frac{Lb}{In^2}\right)$
1	25.6	.01053	2430
2	11.9	.00706	1685
**3	21.0	.00785	2680
4	13.5	.00631	2140
5	18.9	.00950	1990
6	9.9	.00559	1770
7	17.2	.00785	2190
8	15.4	.00785	1960
9	22.0	.0104	2120

RUN #3 Au in O_2 at 1100°C For 1 Hour 10 Min

No	Pull (Lbs)	Area (In^2)	Stress $\left(\frac{Lb}{In^2}\right)$
1	10.25	.00560	1830
2	12.30	.00565	2180
3	16.61	.00904	1840
4	24.62	.0114	2160
5	9.91	.00427	2320
**6	21.0	.0104	2020
7	34.4	.0133	2590
**8	19.14	.00708	2710
9	22.41	.00785	2860

RUN #4 Au in N_2 at 1100°C For 2 Hours 10 Min

No	Pull (Lbs)	Area (In^2)	Stress $\left(\frac{Lb}{In^2}\right)$
1	7.16	.00950	755
2	17.59	.00785	2240
3	10.41	.00636	1640
4	3.30	.00526	630
5	16.60	.00706	2360
6	9.46	.00504	1870
7	5.40	.00427	1260
8	12.60	.00785	1600
**9	30.00	.0122	2450

RUN #5 Au in N_2 at 1100°C For 1 Hour 40 Min

No	θ	Pull (Lbs)	Area (In^2)	Stress $\left(\frac{Lb}{In^2}\right)$
1	130°	9.5	.00706	1350
2	130°	14.7	.00785	1870
3	120°	6.6	.00565	1160
4	120°	8.2	.00785	1040
5	125°	7.0	.00504	1380
6	125°	10.1	.00785	1290

RUN #6 Au in N_2 at 1100°C For 2 Hours 10 Min

No	Pull(Lbs)	Area (In^2)	Stress $\left(\frac{Lb}{In^2}\right)$
1	10.2	.00440	2320
2	4.4	.00384	1150
3	12.9	.00785	1640
**4	7.55	.00440	1710
5	15.6	.00785	1990
6	9.3	.00785	1180.
7	14.7	.00565	2600
8	7.7.	..00565	1360
9	12.5	.00565	2210

RUN #7 Au in N_2 and O_2 at 1100°C For 1 Hour

No	Pull (Lbs)	Area (In^2)	Stress $\left(\frac{Lb}{In^2}\right)$
1	17.1	.00821	2080
2	7.6	.00785	969
3	11.5	.00785	1470
4	13.0	.00864	1510
5	16.3	.00864	1890
6	14.0	.00821	1700
7	14.9	.00833	1790
8	13.8	.00785	1760
9	13.0	.00706	1840

RUN #8 Au in N_2 and O_2 at 1100°C For 1 Hour

No	θ	Pull (Lbs)	Area (In^2)	Stress $\left(\frac{Lb}{In^2}\right)$
1	130°	13.5	.00785	1720
2	130°	11.2	.00706	1580
3	130°	11.5	.00741	1550

RUN #9 Au in N_2 and O_2 at 1100°C For 1 Hour

No	θ	Pull (Lbs)	Area (In^2)	Stress $\left(\frac{Lb}{In^2}\right)$
1	130°	10.8	.00785	1380
2	135°	9.73	.00826	1180
3	130°	9.05	.00826	1090
4	130°	12.1	.00826	1460
5	125°	6.94	.00785	884
6	130°	8.2	.00636	1290
7	120°	8.95	.00826	1080
8	130°	9.55	.00741	1290

RUN #10 Au in O_2 at 1100°C For 9 Hours 20 Min

No	θ	Pull (Lbs)	Area (In^2)	Stress $\left(\frac{Lb}{In^2}\right)$
1	130°	20.9	.00864	2420
2	130°	29.2	.00706	4140
**3	125°	25.3	.00785	3220
4	125°	39.6	.00785	5050
5	125°	24.6	.00950	2590
6	130°	36.2	.00785	4610
** *7	130°	62.6	.00785	7990
8	120°	27.8	.00785	3550
9	120°	60.2	.01130	5320
10	125°	42.3	.00785	5380
**11	125°	34.9	.00950	3680

RUN #11 Au in O_2 at 1100°C For 7 Hours 30 Min

No	Pull (Lbs)	Area (In^2)	Stress $\left(\frac{Lb}{In^2}\right)$
1	30.8	.00671	4590
*2	30.4	.00412	7380
**3	16.6	.00636	2610
**4	27.5	.00785	3500
5	30.0	.00864	3470
6	34.6	.00906	4860
7	25.2	.00864	2920
8	30.4	.00785	3880
**9	5.3	.00565	935

RUN #12 Au in O_2 at 1100°C For 4 Hours 10 Min

No	Pull (Lbs)	Area (In^2)	Stress $\left(\frac{Lb}{In^2}\right)$
**1	27.3	.00706	3860
2	15.9	.00636	2500
3	27.7	.00906	3060
4	30.2	.00864	3500
5	23.4	.00706	3320
*6	57.0	.00950	6000
7	25.0	.00950	2630
**8	23.1	.00864	2680

RUN #13 Au in O_2 at 1200°C For 1 Hour 35 Min

No	Pull (Lbs)	Area (In^2)	Stress $\left(\frac{Lb}{In^2}\right)$
1	12.1	.00636	1900
**2	28.2	.00706	3990
**3	4.18	.00671	622
4	41.3	.00906	4560
**5	42.2	.00950	4450
6	46.2	.00994	4670
7	29.5	.00864	3420
*8	50.9	.00950	5360
**9	15.6	.00950	1640

RUN #14 Au in O_2 at 1200°C For 1 Hour 25 Min

No	Pull (Lbs)	Area (In^2)	Stress $\left(\frac{Lb}{In^2}\right)$
1	79.6	.0104	7660
**2	52.3	.00864	6060
**3	30.2	.00864	3500
**4	22.2	.00746	2970
**5	32.9	.00432	7610
* **6	92.7	.00950	9750
7	30.8	.00785	3920

RUN #15 Au in O_2 at 1200°C For 2 Hours 45 Min

No	Pull (Lbs)	Area (In^2)	Stress $\left(\frac{Lb}{In^2}\right)$
1	24.2	.00742	3260
2	29.5	.00950	3110
**3	33.0	.0104	3170
4	31.6	.00950	3320
5	26.6	.00824	3230
*6	53.7	.00950	5660

RUN #16 Au in O_2 at 1200°C For 1 Hour 55 Min

No	Pull (Lbs)	Area (In^2)	Stress $\left(\frac{Lb}{In^2}\right)$
*1	19.45	.00504	3860
**2	30.6	.00864	3540
**3	18.2	.00824	2210
**4	21.45	.00824	2610
5	18.05	.00864	2090
**6	12.8	.00944	1360

RUN #17 Au in O_2 at 1200°C For 2 Hours 10 Min

No	Pull (Lbs)	Area (In^2)	Stress $\left(\frac{Lb}{In^2}\right)$
**1	41.6	.00994	4180
**2	16.1	.00746	2160
3	15.2	.00452	3360
*4	44.0	.00864	5100
**5	12.5	.00534	2340
6	14.0	.00636	2200

RUN #18 Au in O_2 at 1200°C For 1 Hour

No	Pull (Lbs)	Area (In^2)	Stress $\left(\frac{Lb}{In^2}\right)$
**1	24.55	.00706	3470
2	17.88	.00504	3540
**3	29.05	.00440	6600
*4	70.0	.00994	7040
**5	45.2	.00824	5490
6	47.8	.00746	6410

RUN #19 Au in O_2 at 1150°C For 1 Hour

No	Pull (Lbs)	Area (In^2)	Stress $\left(\frac{Lb}{In^2}\right)$
**1	7.92	.00706	1120
**2	22.8	.00934	2440
3	17.15	.00565	3030
**4	11.45	.00864	1330
*5	27.7	.00600	4610
6	8.85	.00535	1650
**7	20.2	.00778	2590
8	20.9	.00864	2420
9	12.89	.00785	1640

RUN #20 Au in O_2 at 1150°C For 2 Hours 8 Min

No	Pull (Lbs)	Area (In^2)	Stress $\left(\frac{Lb}{In^2}\right)$
1	15.39	.00535	2880
* **2	27.2	.00648	4200
3	17.6	.00600	2940
**4	29.0	.00785	3700
5	15.88	.00825	1920
**6	9.27	.00600	1540
7	30.25	.0122	2480
8	28.3	.00825	3430
**9	23.5	.00706	3330

RUN #21 Au in O_2 at 1150°C For 6 Hours 40 Min

No	Pull (Lbs)	Area (In^2)	Stress $\left(\frac{Lb}{In^2}\right)$
1	24.62	.00600	4110
2	24.1	.00785	3070
**3	23.95	.00671[a]	3560
*4	20.4	.00267	7620
5	33.65	.00825	4080
6	32.85	.00825	3980
**7	17.0	.00864	1970

RUN #22 Au in O_2 at 1150°C For 4 Hours 30 Min

No	Pull (Lbs)	Area (In^2)	Stress $\left(\frac{Lb}{In^2}\right)$
1	12.7	.00668	1900
2	24.0	.00636	3770
**3	26.4	.00825	3200
4	23.8	.00535	4440
5	32.0	.00950	3370
*6	41.0	.00864	4740
7	32.45	.00785	4130

RUN #23 Au in O_2 at 1150°C For 1 Hour 30 Min

No	Pull (Lbs)	Area (In^2)	Stress $\left(\frac{Lb}{In^2}\right)$
1	16.3	.00565	2880
* **2	16.8	.00504	3340
3	26.3	.00864	3040
**4	18.24	.00825	2210
5	19.3	.00785	2460
6	22.0	.00785	2800
7	11.26	.00785	1430

RUN #24 Au in O_2 at 1150°C For 1 Hour 10 Min

No	Pull (Lbs)	Area (In^2)	Stress $\left(\frac{Lb}{In^2}\right)$
1	19.8	.00785	2520
2	23.1	.00785	2940
*3	30.2	.00825	3660
4	16.95	.00785	2060

RUN #25 Au in O_2 at 1150°C For 1 Hour 23 Min

No	Pull (Lbs)	Area (In^2)	Stress $\left(\frac{Lb}{In^2}\right)$
1	19.8	.00785	2520
2	25.0	.00785	3180
*3	28.0	.00745	3760
4	20.75	.00745	2780
5	20.55	.0113	1820

BIBLIOGRAPHY

1. Presnova, N. A., "Physicochemical Nature of Bonds Between Dissimilar Materials," Siberian Physicotechnical Scientific-Research Institute.

2. Brace, Porter H., "Reactions of Molten Titanium with Certain Refractory Oxides," J. Electrochem. Soc., Vol. 94, No. 4 (1948), pp. 170 - 176.

3. Bondi, A., "The Spreading of Liquid Metals on Solid Surfaces; Surface Chemistry of High-Energy Substances," Chem. Revs., Vol. 52, No. 2 (1953), pp. 417 - 458.

4. Economos, George, "Behavior of Refractory Oxides in Contact with Metals at High Temperatures," Industrial and Engineering Chemistry, Vol. 45 (1953), pp. 458 - 459.

5. Economos, G., and Kingery, W. D., "Metal-Ceramic Interactions: II Metal Oxide Interfacial Reactions at Elevated Temperatures," J. Am. Ceram. Soc., Vol. 36, No. 12 (1953), pp. 403 - 409.

6. Norton, F. H., Kingery, W. D., Economos, G., and Humenik, M., Jr., "Study of Metal-Ceramic Interactions at Elevated Temperatures," USAEC Report Number NYO-3144, Feb., 1953.

7. Pincus, A. G., "Mechanism of Ceramic-to-Metal Adherence--Adherence of Molybdenum to Alumina Ceramics," Ceramic Age, March, 1954, pp. 16 - 33.

8. Livey, D. T., and Murray, P., "The Wetting Properties of Solid Oxides and Carbides by Liquid Metals," PLANSEE Proceedings, Chapter 32 (1955), pp. 375 - 404.

9. Kingery, W. D., "Role of Surface Energies and Wetting in Metal/Ceramic Sealing," Ceramic Bulletin, Vol. 35, No. 3 (1956), pp. 108 - 112.

10. Van Houten, G. R., "A Survey of Ceramic-to-Metal Bonding," Ceramic Bulletin, Vol. 38, No. 6 (1959), pp. 301 - 307.

11. Williams, J. C., and Nielsen, J. W., "Wetting of Original and Metallized High Alumina Surfaces by Molten Brazing Solder," J. Amer. Ceram. Soc., Vol. 42, No. 5 (1959), pp. 229 - 235.

12. Denton, E. P., and Rawson, H., "The Metallizing of High Al_2O_3 Ceramics," Trans. Britt Ceram. Soc., Vol. 59, No. 2 (1960), pp. 25 - 37.

13. Cole, Sandford S., Jr., and Inge, John E., "Calculation and Measurement of Stress in Ceramic-to-Metal Seal," Ceramic Bulletin, Vol. 40, No. 12 (1961), pp. 738 - 743.

14. Cole, S. S., and Sommer, G., "Glass Migration Mechanism of Ceramic-to-Metal Seal Adherence," J. Am. Ceram.Soc., Vol. 44, No. 6 (1961), pp. 265 - 271.

15. Floyd, James R., "Effect of Composition and Crystal Size of Alumina Ceramics on the Metal-to-Ceramic Bond Strength," Ceramic Bulletin, Vol. 42, No. 2 (1963), pp. 65 - 70.

16. Kohl, W. H., "Ceramics and Ceramic-to-Metal Sealing," Vacuum, Vol. 14, No. 9 (1964), pp. 333 - 354.

17. Porembka, Stanley W., Jr., "Joining Ceramics to Metals for High Temperature Service," Battelle Tech. Rev., Vol. 13, No. 9 (1964), pp. 2 - 7.

18. Reed, Leonard, and Huggins, R. A., "Electron Probe Microanalysis of Ceramic-to-Metal Seals," J. Am. Ceram. Soc., Vol. 48, No. 8 (1965), pp. 421 - 426.

19. Van Vlack, L.H.,"The Metal-Ceramic Boundary," Metals Engineering Quarterly, ASM, Nov., 1965, pp. 7 - 12.

20. Helgesson, C. I., "Investigation of the Bonding Mechanism Between Metals and Ceramics: I Ceramic-to-Metal Seals," Chalmers Tekniska Hogskolas Handlingar (Transactions of Chalmers University of Technology, Gottenburg, Sweden), 1966.

21. Patter, H. E., Evans, R. M., and Monroe, R. E., "Joining Ceramics and Graphite to Other Materials," NASA Report No. SP-5052 (1968).

22. Kingery, W. D., and Humenik, M., Jr., "Surface Tension at Elevated Temperatures: I Furance and Method for Use of the Sessile Drop Method; Surface Tension of Silicon, Iron, and Nickel," J. Phys. Chem., Vol. 57, (1953), pp. 359 - 363.

23. Humenik, Michael, Jr., and Kingery, William D., "Metal-Ceramic Interactions: III Surface Tension and Wettability of Metal-Ceramic Systems," J. Am. Ceram. Soc., Vol. 37, No. 1 (1954), pp. 18 - 23.

24. Kingery, W. D., "Metal-Ceramic Interactions: IV Absolute Measurement of the Metal-Ceramic Interfacial Energy and the Interfacial Adsorption of Silicon from Iron-Silicon Alloys," J. Am. Ceram. Soc., Vol. 37, No. 2 (1954), pp. 42 - 45.

25. Halden, F. A., and Kingery, W. D., "Surface Tension at Elevated Temperatures: II Effect of C, N, O, and S on Liquid Iron Surface Tension and Interfacial Energy with Al_2O_3," J. Phys. Chem., Vol. 59 (1955), pp. 557 - 559.

26. Kurkjian, C. R., and Kingery, W. D., "Surface Tension at Elevated Temperatures: III Effect of Cr, In, Sn, and Ti on Liquid Nickel Surface Tension and Interfacial Energy with Al_2O_3," J. Phys. Chem., Vol. 60, No. 7 (1956), pp. 961 - 963.

27. Allen, B. C., and Kingery, W. D., "Surface Tension and Contact Angles in Some Liquid Metal-Solid Ceramic Systems at Elevated Temperatures," Trans. Met. Soc. AIME, Vol. 215, Feb., 1959, pp. 30 - 37.

28. Armstrong, W. M., Chaklader, A. C. D., and Clarke, J. F., "Interface Reactions Between Metals and Ceramics: I Sapphire-Nickel Alloys," J. Am. Ceram. Soc., Vol. 45, No. 3 (1962), pp. 115 - 118.

29. Sutton, W. H., and Chorne, J., "Development of High Strength, Heat Resistant Alloys by Whisker Reinforcement," Metals Engineering Quarterly, Vol. 3, No. 1 (1963), pp. 44 - 51.

30. Sutton, W. H., "Investigation of Oxide-Fiber (Whisker) Reinforced Metals," Technical Report AMRA CR63-01/8 (Final Report), June, 1964.

31. Sutton, Willard H., and Feingold, Earl, "Investigation of Bonding in Oxide-Fiber (Whisker) Reinforced Metals," Technical Report AMRA CR65-01/4 (Final Report), July, 1965.

32. Sutton, Willard H., and Feingold, Earl, "Role of Interfacially Active Metals in the Apparent Adherence of Nickel to Sapphire," Materials Science Research, Vol. 3 (1966), pp. 577 - 611.

33. Forgan, R. R. D., Nicholas, M., and Poole, D. M., "The Adhesion of Metal/Alumina Interfaces," J. Mat. Sci., Vol. 3 (1968), pp. 9 - 14.

34. Nicholas, M., "The Strength of Metal/Alumina Interfaces," J. Mat. Sci., Vol. 3 (1968), pp. 571 - 576.

35. Benjamin, P., and Weaver, C., "Condensation Energies for Metals on Glass and Other Substrates," Proc. Roy. Soc., A, Vol. 252 (1959), pp. 418 - 430.

36. Weaver, C., and Hill, R. M., "Aging Effects in Bimetallic Films," Phil. Mag., 1959, pp. 1107 - 1125.

37. Benjamin, P., and Weaver, C., "Measurement of Adhesion of Thin Films," Proc. Roy. Soc., A, Vol. 254 (1960), pp. 163 - 176.

38. Benjamin, P., and Weaver, C., "Adhsion of Metal Film to Glass," Proc. Roy. Soc., Vol. 254 (1960), pp. 177 - 183.

39. Benjamin, P., and Weaver, C., "The Adhesion of Evaporated Metal Films on Glass," Proc. Roy. Soc., A, Vol. 261 (1961), pp. 516 - 531.

40. Bowie, M. H., "Bond Strength of Evaporated Thin Metal Films on Glass," Master's Thesis, Lehigh University, Bethlehem, Pa., January 11, 1963.

41. Benjamin, P., and Weaver, C., "The Adhesion of Metals to Crystal Faces," Proc. Roy. Soc., A, Vol. 274 (1963), pp. 267 - 273.

42. Strverding, B., "The Bond in Heterogeneous Interfaces," J. Electrochem. Soc., July, 1963, pp. 712 - 716.

43. Karnowsky, M. M., and Estell, W. B., "Scratch Test for Measuring Adherence of Thin Films to Oxide Substrates," Rev. Sci. Inst., Vol. 35, No. 10 (1964), pp. 1324 - 1326.

44. Mattox, D. M., "Metallizing Ceramics Using a Gas Discharge," Sandia Corp., Reprint #SC-R-64-1330, September, 1964.

45. Mattox, D. M., "Interface Formation and the Adhesion of Thin Films," Sandia Corporation Monograph No. SC-R-65-852, January, 1965.

46. Weaver, C., "The Adhesion of Metal Films to Surfaces," Chemistry and Industry, Feb. 27, 1965, pp. 370 - 373.

47. Beno, R. L., "An Adhesion Tester for Evaporated Metal Films," NASA Technical Report #N66-25360, Jan., 1966.

48. Mattox, D. M., "Influence of Oxygen on the Adherence of Gold Films to Oxide Substrates," J. App. Phys., Vol. 37, No. 9 (1966), pp. 3613 - 3615.

49. Moore, D. G., and Thornton, H. R., "Effect of Oxygen on the Bonding of Gold to Fused Silica," Journal of Research of the National Bureau of Standards, Vol. 62, No. 3 (1959), pp. 127 - 135.

50. Pilliar, R. M., and Nutting, J., "Solid-Solid Interfacial Energy Determinations in Metal-Ceramic Systems," Phil. Mag., Vol. 16 (1967), p. 181.

51. Carpenter, L. G., and Mair, W. N., "Reaction Between Oxygen and Hot Gold," Nature, Vol. 179 (1957), p. 212.

52. Shewmon, Paul G., Diffusion in Solids, New York: McGraw-Hill Book Company, 1963.

53. Crank, J., Mathematics of Diffusion, London: Oxford University Press, 1956.

54. Oishi, Y., and Kingery, W. D., "Self-Diffusion of Oxygen in Single Crystal and Polycrystalline Aluminum Oxide, "Journal of Chemical Physics, Vol. 33, No. 2 (1960).

VITA

James LeRoy Brandner, son of Wilbur L. and Beatrice B. (Hight) Brandner, was born June 24, 1942, in Spring Valley, Illinois. He graduated from Hall High School in 1960 and enrolled at Illinois State University as a mathematics major. In 1962 he transferred to the University of Illinois where he graduated in 1965 with a BSEE.

In 1965 he was employed by the Western Electric Company as an engineer in capacitor design and development engineering at the company's Hawthorne Works in Cicero, Illinois. In 1966 he was promoted to development engineer and in 1967 he was transferred to the Engineering Research Center at Princeton, New Jersey, where he was assigned to the ceramics processing department as a participant in the Western Electric Lehigh Master's Degree Program.

The author is married to Annette K. (Butcher) Brandner and is the father of a son, Michael S. Brandner, aged 6 months.